8th U.S. National Congress on Computational Mechanics

A Posteriori Error Estimation and Adaptive Procedures from 1976 to 2005.

High Accuracy Simulations of Resistivity Logging Instruments Using a Self-Adaptive Goal-Oriented hp Finite Element Method

David Pardo (dzubiaur@yahoo.es),
L. Demkowicz, C. Torres-Verdin

Collaborators: Science Department of Baker-Atlas,
L. Tabarovsky, J. Kurtz, M. Paszynski, D. Xue

July 27, 2005

Department of Petroleum and Geosystems Engineering, and
Institute for Computational Engineering and Sciences (ICES)
The University of Texas at Austin

OVERVIEW

1. Motivation: Simulation of Resistivity Logging Instruments.
2. Methodology:
   - The hp-Finite Element Method (FEM).
   - Self-Adaptive hp-FEM.
   - Self-Adaptive Goal-Oriented hp-FEM.
3. Numerical Results:
   - Simulation of Resistivity Logging Instruments with Casing.
   - Simulation of Resistivity Logging Instruments with Mandrel.
4. Conclusions and Future Work (3D Problems, Multi-physics).

RESISTIVITY LOGGING INSTRUMENTS

Logging Instruments: Definition

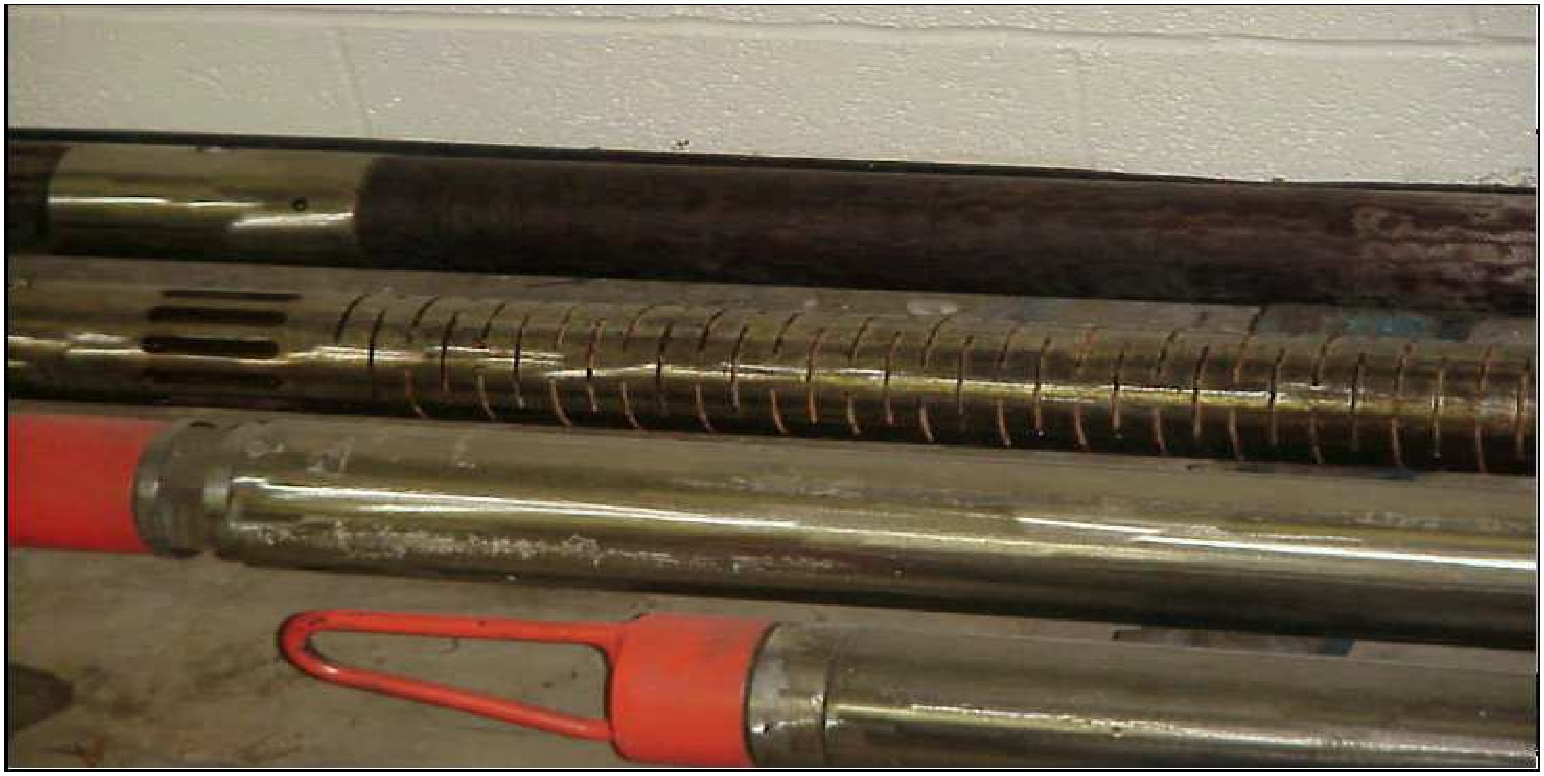

RESISTIVITY LOGGING INSTRUMENTS

Utility of Logging Instruments

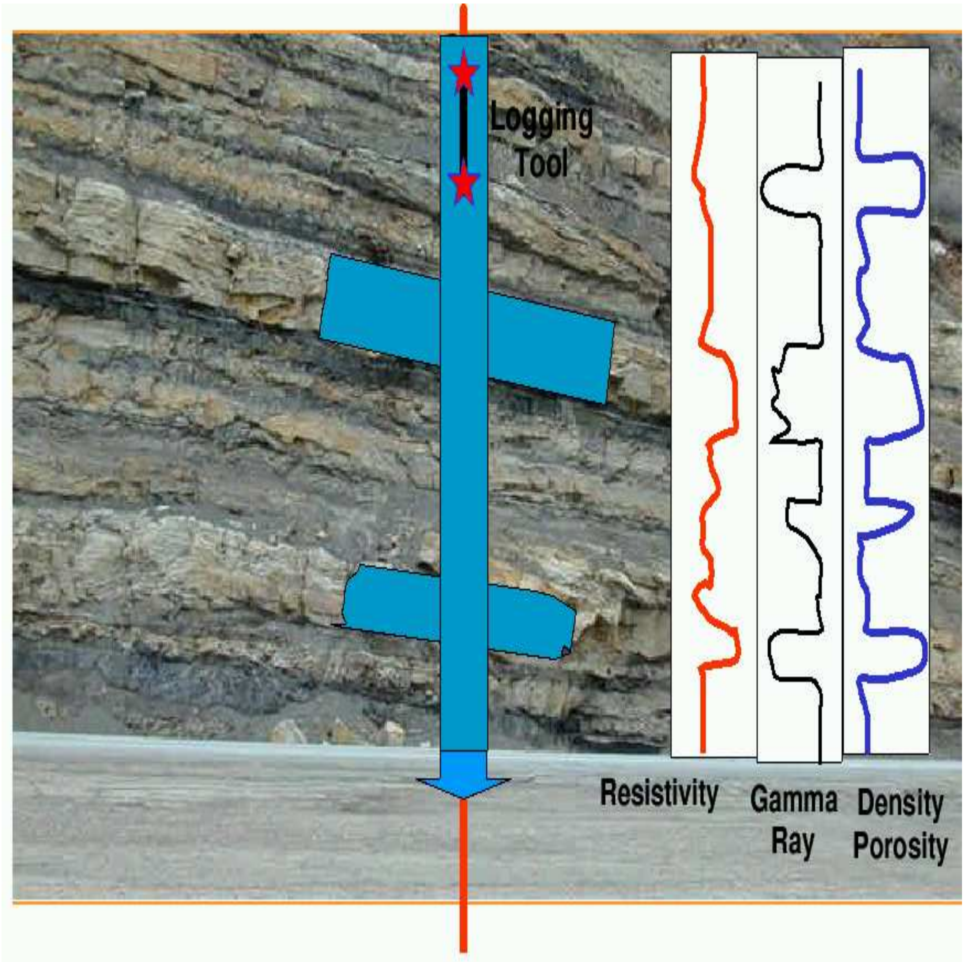

OBJECTIVES: To determine

- **Payzones (oil and gas).**
- **Amount of oil/gas.**
- **Ability to extract oil/gas.**

$

RESISTIVITY LOGGING INSTRUMENTS

Main Objective: To Solve an Inverse Problem

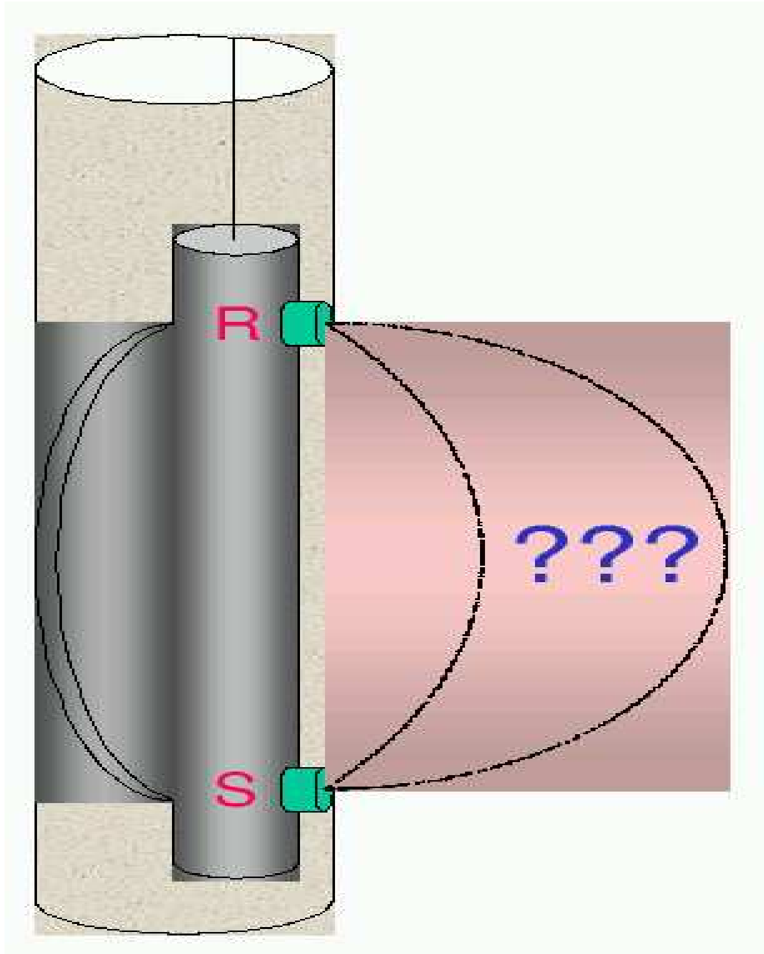

A software for solving the DIRECT problem is essential in order to solve the INVERSE problem

RESISTIVITY LOGGING INSTRUMENTS

Resistivity Logging Instruments

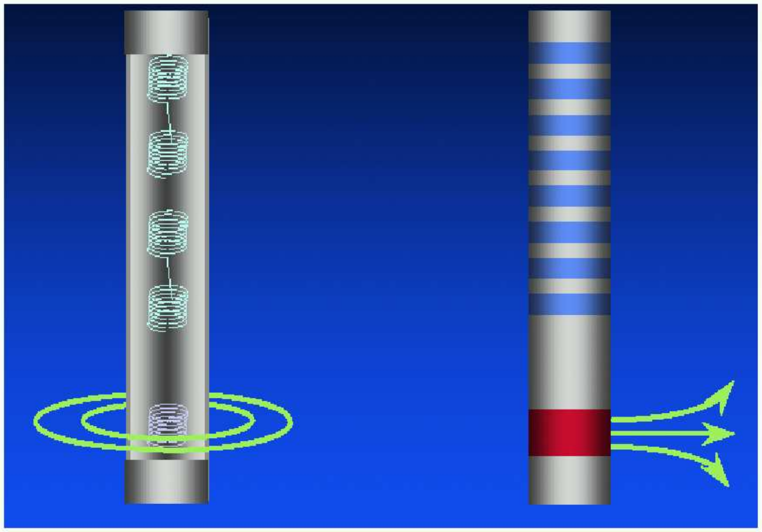

RESISTIVITY LOGGING INSTRUMENTS

Final Result Obtained from the Logging Instruments

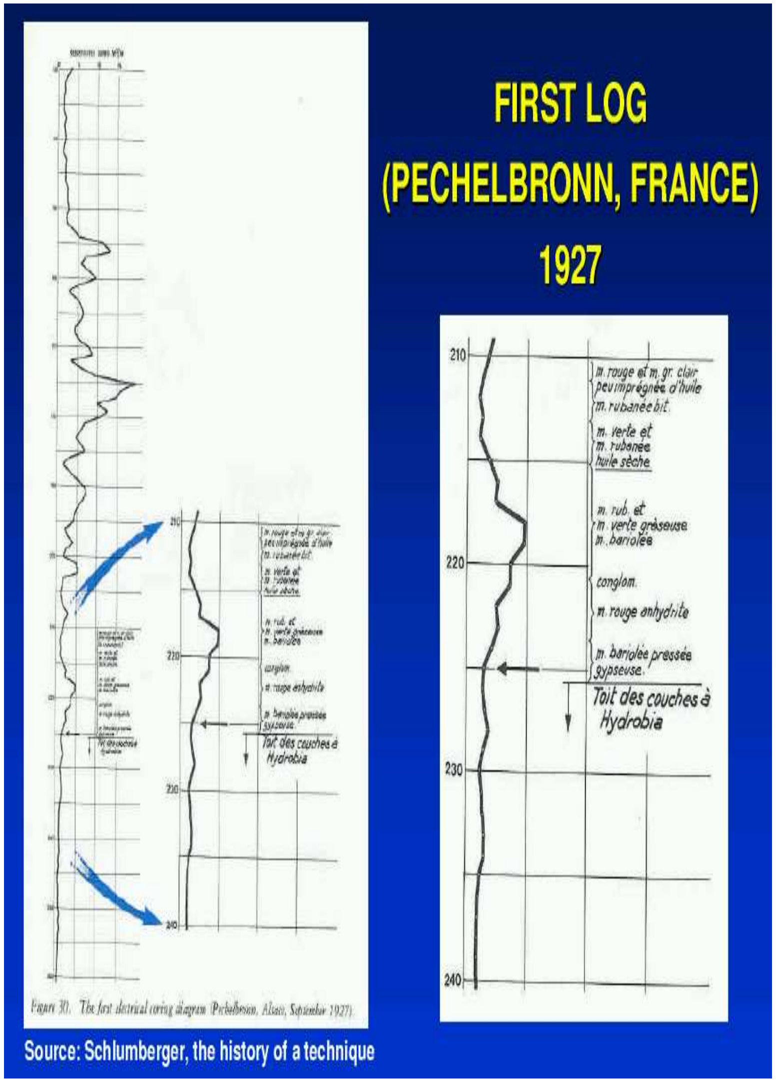

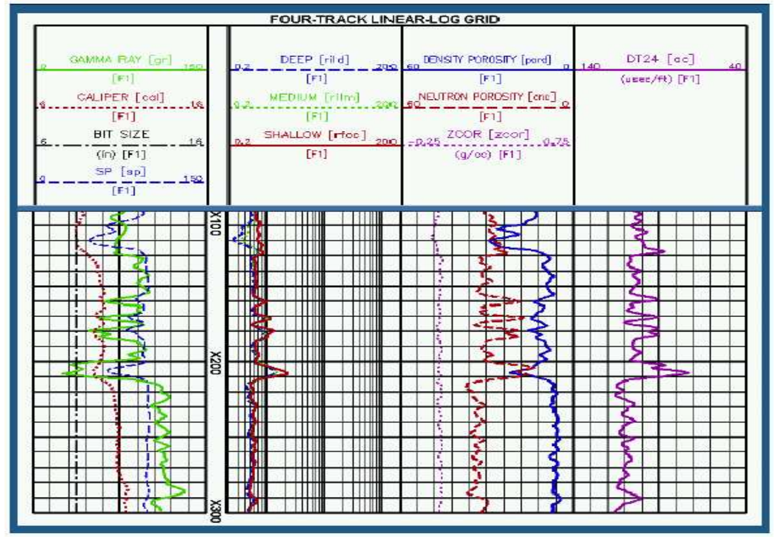

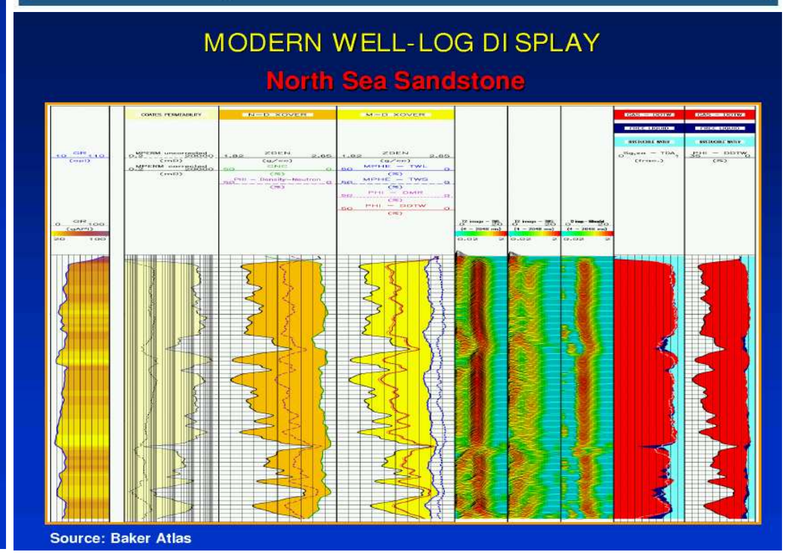

RESISTIVITY LOGGING INSTRUMENTS

Model Problem with Steel Casing

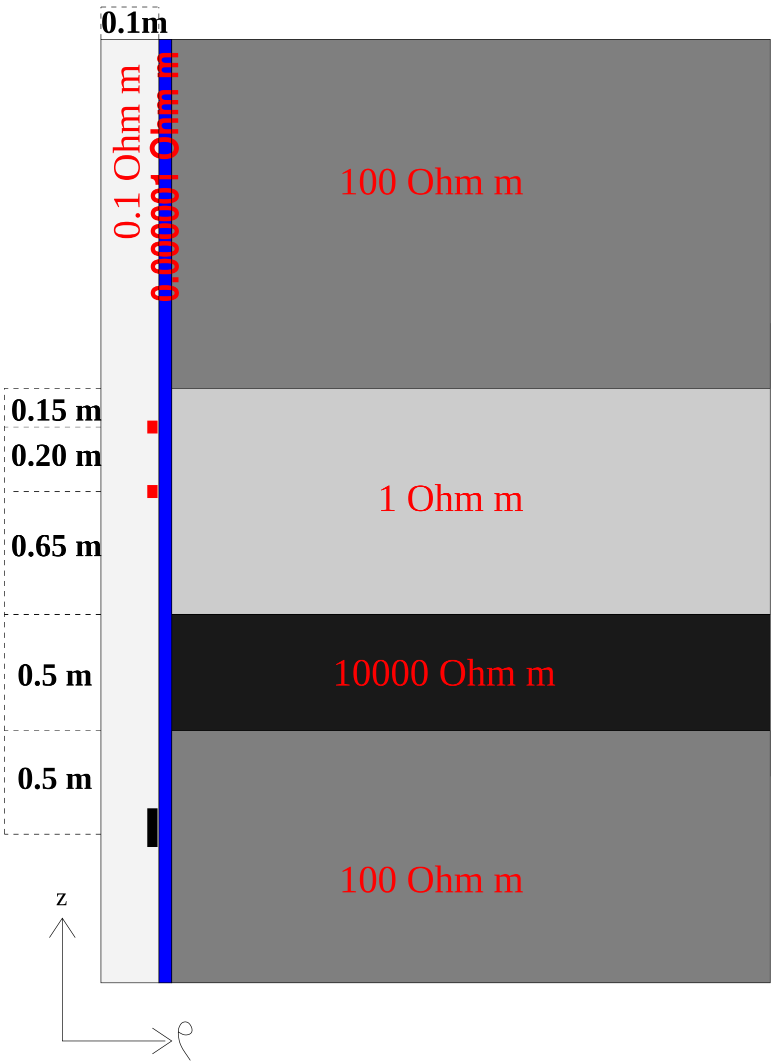

Frequency: 10 Hz - 10 kHz.

Casing resistivity: 10^{-6} Ohm · m.

Casing width: 0.01127 m

Discretization error $<$ 0.1 $\%$

Toroidal antennas

Size (domain): 500m x 4000m

THE hp-FINITE ELEMENT METHOD (FEM)

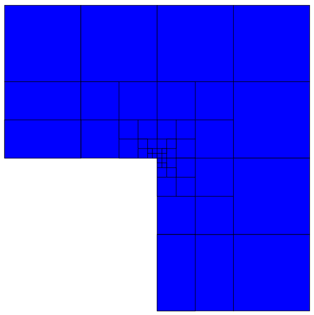

The h-Finite Element Method

1. Convergence limited by the polynomial degree, and large material contrasts.
2. Optimal *h*-grids do NOT converge exponentially in real applications.
3. They may "lock" (100$\%$ error).

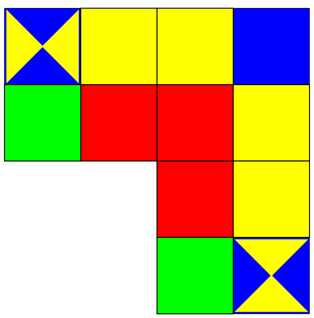

The p-Finite Element Method

1. Exponential convergence feasible for analytical ("nice") solutions.
2. Optimal *p*-grids do NOT converge exponentially in real applications.
3. If initial *h*-grid is not adequate, the *p*-method will fail miserably.

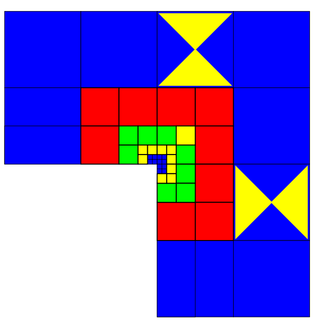

The hp-Finite Element Method

1. Exponential convergence feasible for ALL solutions.
2. Optimal *hp*-grids DO converge exponentially in real applications.
3. If initial *hp*-grid is not adequate, results will still be great.

SELF-ADAPTIVE hp-FEM

Energy norm based fully automatic *hp*-adaptive strategy

Coarse grids (hp) **Fine grids** $(h/2, p+1)$

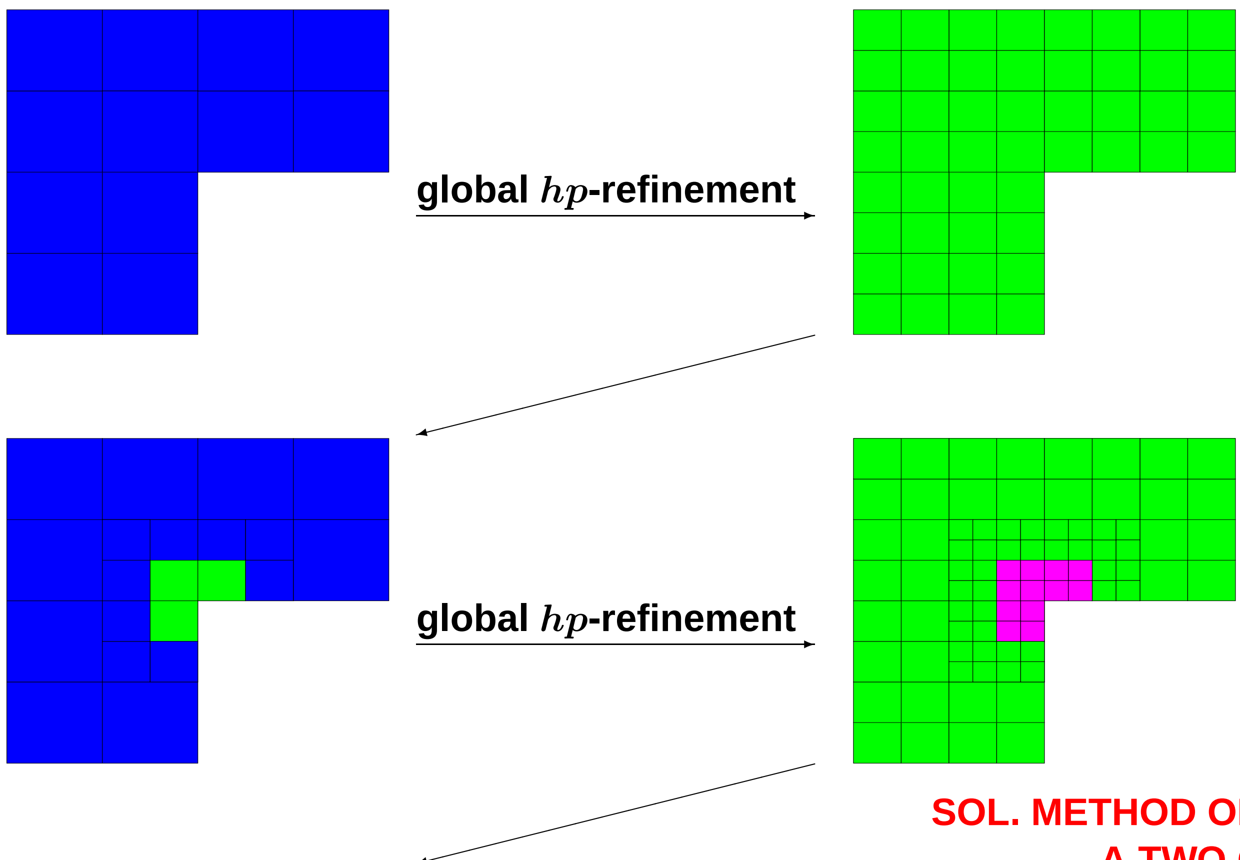

SOL. METHOD ON FINE GRIDS:
A TWO GRID SOLVER

SELF-ADAPTIVE GOAL-ORIENTED hp-FEM

Motivation (Goal-Oriented Adaptivity)

Test Problem

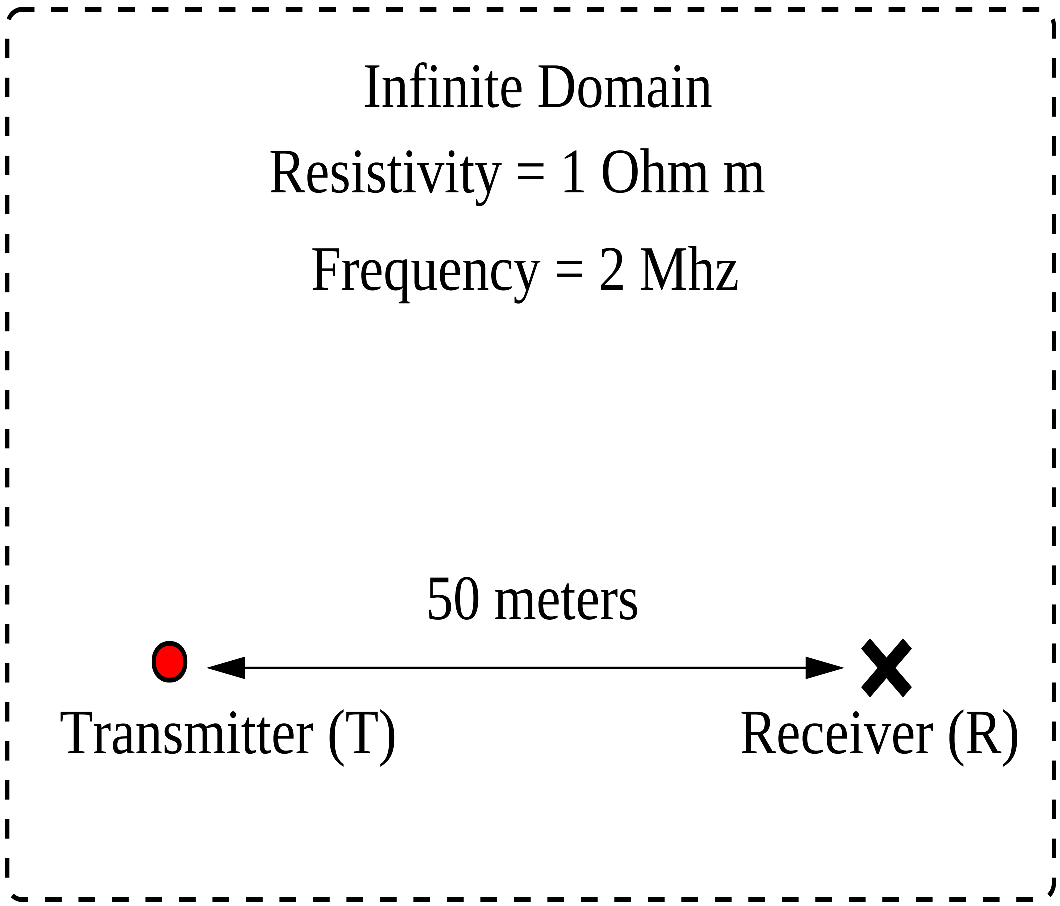

SELF-ADAPTIVE GOAL-ORIENTED hp-FEM

Motivation (Goal-Oriented Adaptivity)

Test Problem

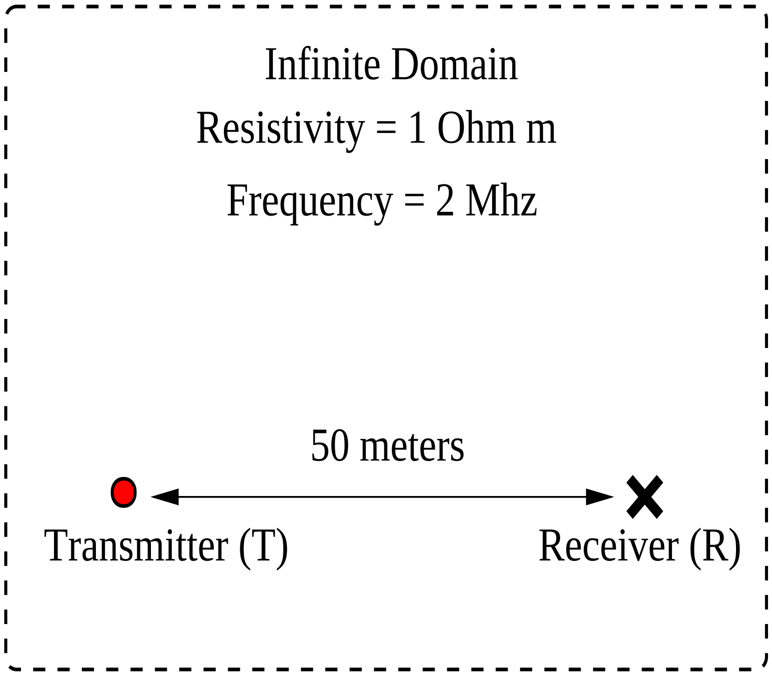

- **Solution decays exponentially.**
- $\dfrac{|\boldsymbol{E(T)}|}{|\boldsymbol{E(R)}|} \approx 10^{60}$
- **Results using energy-norm adaptivity:**
  - **Energy-norm error:** 0.001%
  - **Relative error in the quantity of interest** $> 10^{30}$ $\%$.

SELF-ADAPTIVE GOAL-ORIENTED hp-FEM

Motivation (Goal-Oriented Adaptivity)

Test Problem

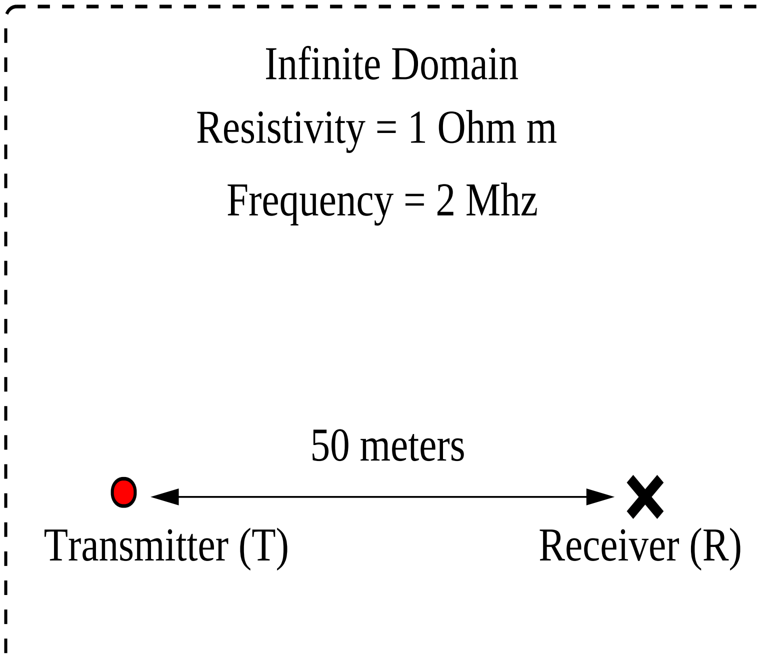

- **Solution decays exponentially.**
- $\dfrac{|E(T)|}{|E(R)|} \approx 10^{60}$
- **Results using energy-norm adaptivity:**
  - **Energy-norm error:** 0.001%
  - **Relative error in the quantity of interest** $> 10^{30}\ \%$.

Goal-oriented adaptivity is needed

Becker-Rannacher (1995,1996), Rannacher-Stuttmeier (1997), Cirak-Ramm (1998), Paraschivoiu-Patera (1998), Peraire-Patera (1998), Prudhomme-Oden (1999, 2001), Heuveline-Rannacher (2003), Solin-Demkowicz (2004).

SELF-ADAPTIVE GOAL-ORIENTED hp-FEM

Motivation (Goal-Oriented Adaptivity)

Test Problem

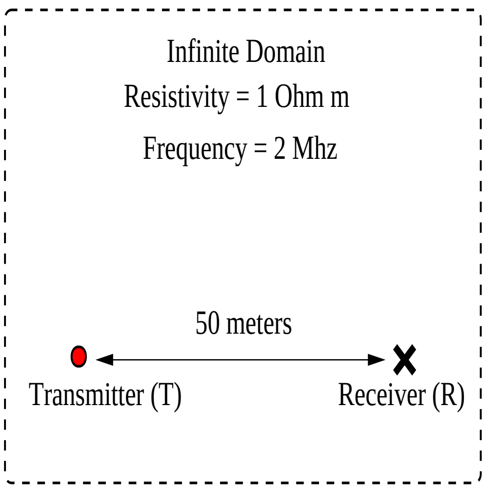

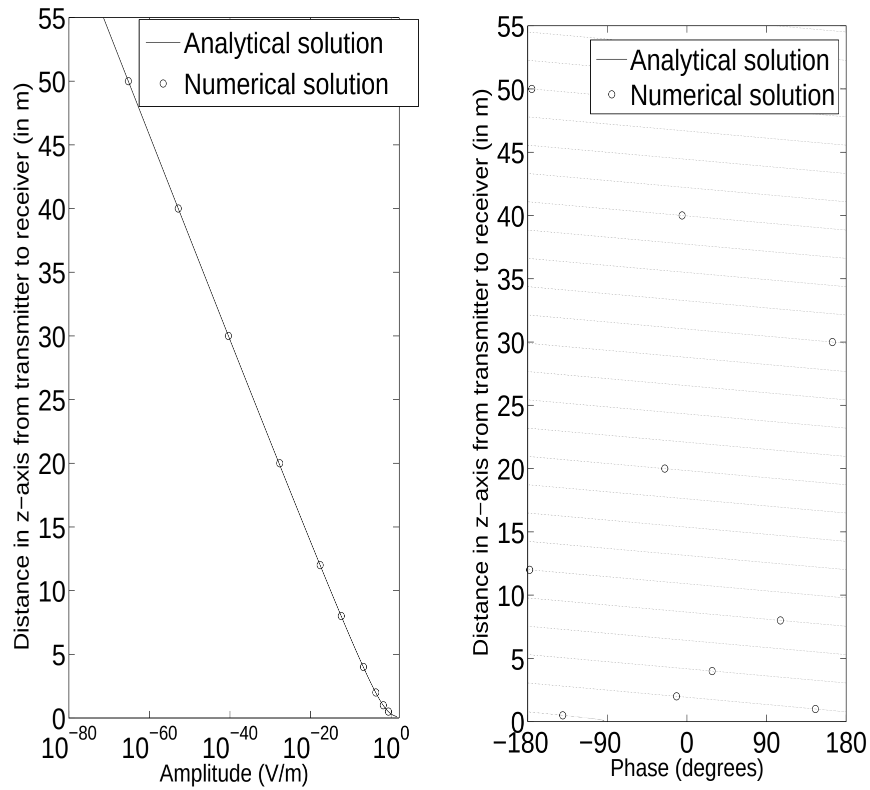

Goal-oriented adaptivity is needed

SELF-ADAPTIVE GOAL-ORIENTED hp-FEM

Mathematical Formulation (Goal-Oriented Adaptivity)

We consider the following problem (in variational form):

$$\left\{\begin{array}{l}\text{Find } L(\Psi)\text{, where } \Psi \in V \text{ such that :}\\ b(\Psi,\xi) = f(\xi) \quad \forall \xi \in V \ .\end{array}\right.$$

We define residual $r_e(\xi) = b(e,\xi)$. We seek for solution G of:

$$\left\{\begin{array}{l}\text{Find } G \in V'' \sim V \text{ such that :}\\ G(r_e) = L(e) \ .\end{array}\right.$$

This is necessarily solved if we find the solution of the *dual* problem:

$$\left\{\begin{array}{l}\text{Find } G \in V \text{ such that :}\\ b(\Psi,G) = L(\Psi) \quad \forall \Psi \in V \ .\end{array}\right.$$

Notice that $L(e) = b(e,G)$.

SELF-ADAPTIVE GOAL-ORIENTED hp-FEM

Mathematical Formulation (Goal-Oriented Adaptivity)

DIRECT PROBLEM

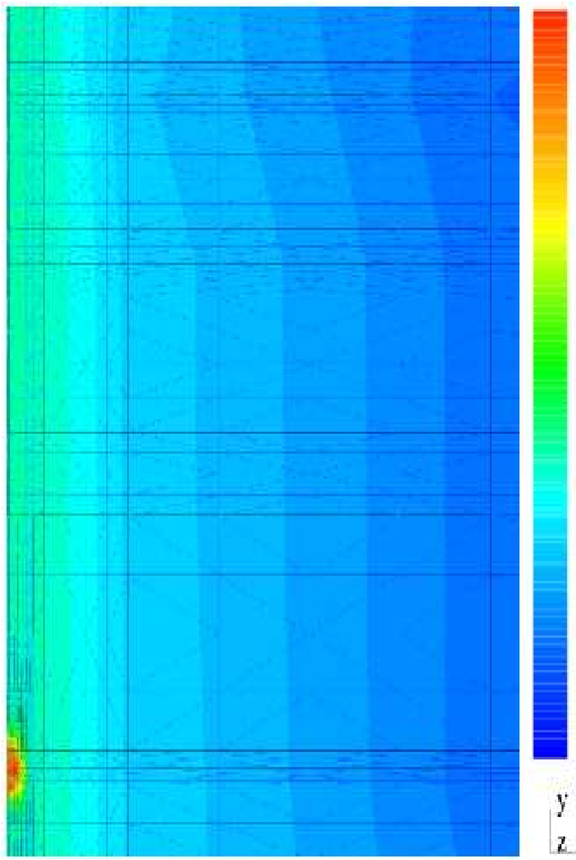

DUAL PROBLEM

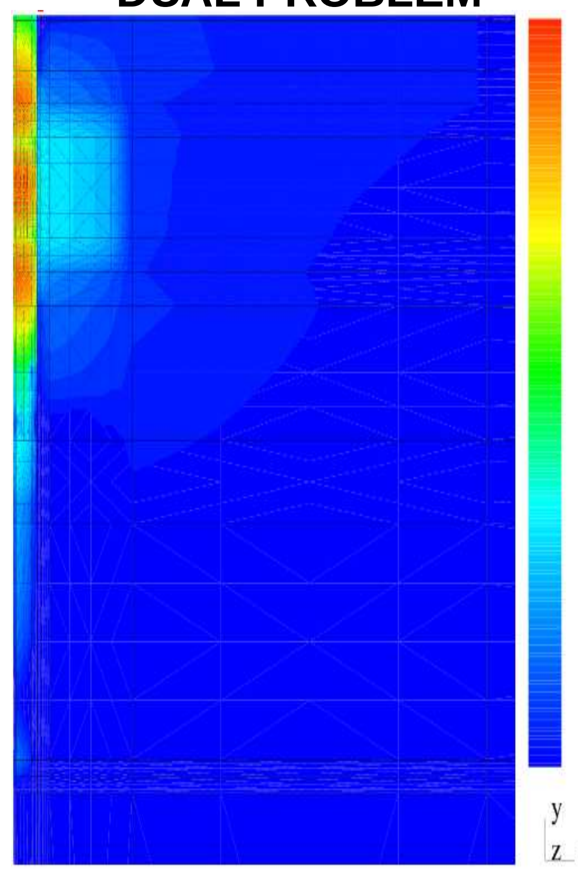

$$L(\Psi)=b(\Psi,G)$$

SELF-ADAPTIVE GOAL-ORIENTED hp-FEM

Algorithm for Goal-Oriented Adaptivity

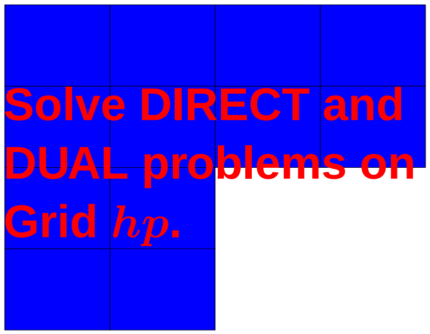

$\longrightarrow$

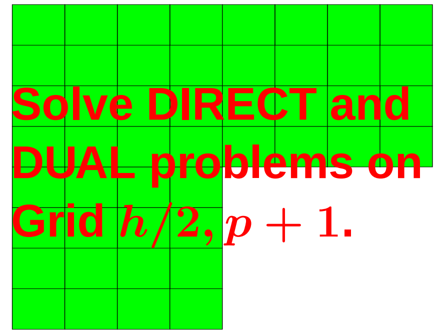

Compute $e = \Psi_{h/2,p+1} - \Psi_{hp}$, **and** $\tilde{e} = \Psi_{h/2,p+1} - \Pi_{hp}\Psi_{h/2,p+1}$.
Compute $\epsilon = G_{h/2,p+1} - G_{hp}$, **and** $\tilde{\epsilon} = G_{h/2,p+1} - \Pi_{hp} G_{h/2,p+1}$.

$$|L(e)| = |b(e,\epsilon)| \sim |b(\tilde{e},\tilde{\epsilon})| \leq \sum_K |b_K(\tilde{e},\tilde{\epsilon})| \leq \sum_K \| \tilde{e} \|_{E,K} \| \tilde{\epsilon} \|_{E,K}.$$

Apply the fully automatic hp-adaptive algorithm.

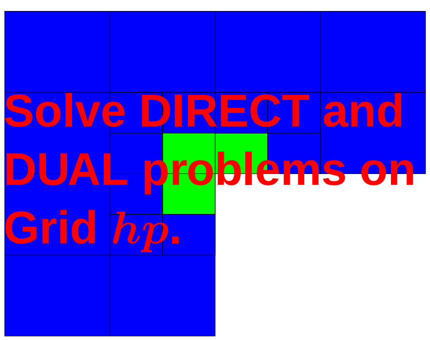

$\longrightarrow$

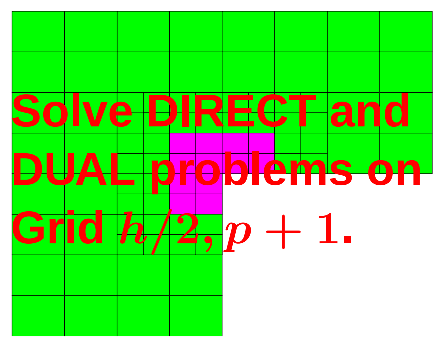

SELF-ADAPTIVE GOAL-ORIENTED hp-FEM

Model Problem with Steel Casing

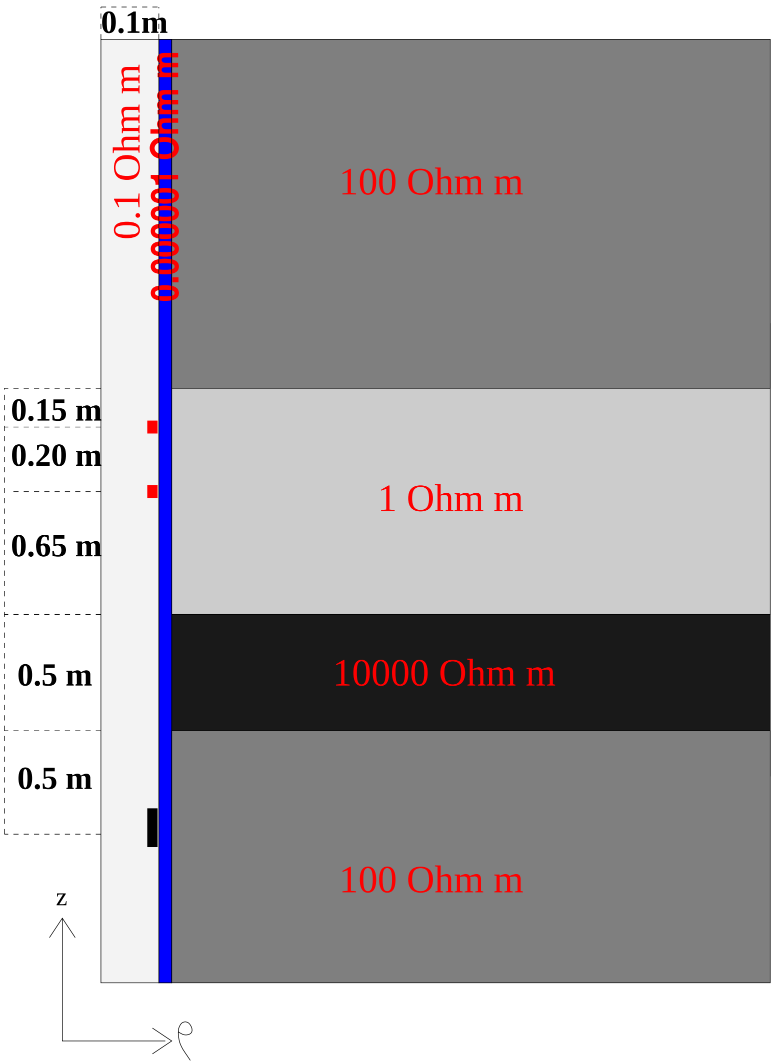

Frequency: 10 Hz - 10 kHz.

Casing resistivity: 10^{-6} Ohm · m.

Casing width: 0.01127 m

Discretization error $<$ 0.1 $\%$

Toroidal antennas

Size (domain): 500m x 4000m

NUMERICAL RESULTS

Electromagnetism

Time-Harmonic Maxwell's Equations

$\nabla \times \mathrm{H} = (\bar{\bar{\sigma}} + j\omega\bar{\bar{\epsilon}})\mathrm{E} + \mathrm{J}^{imp}$	**Ampere's law**
$\nabla \times \mathrm{E} = -j\omega\bar{\bar{\mu}}\mathrm{H} - \mathrm{M}^{imp}$	**Faraday's law**
$\nabla \cdot (\bar{\bar{\epsilon}}\mathrm{E}) = \rho$	**Gauss' law of Electricity**
$\nabla \cdot (\bar{\bar{\mu}}\mathrm{H}) = 0$	**Gauss' law of Magnetism**

E-VARIATIONAL FORMULATION:

$$\left\{ \begin{array}{l} \textbf{Find } \mathrm{E} \in \mathrm{E}_D + H_D(\mathrm{curl};\Omega) \textbf{ such that:} \\ \displaystyle\int_\Omega (\bar{\bar{\mu}}^{-1}\nabla \times \mathrm{E}) \cdot (\nabla \times \bar{\mathrm{F}})\, dV - \int_\Omega (\bar{\bar{k}}^2\mathrm{E}) \cdot \bar{\mathrm{F}}\, dV = -j\omega \int_\Omega \mathrm{J}^{imp} \cdot \bar{\mathrm{F}}\, dV \\ \displaystyle +j\omega \int_{\Gamma_N} \mathrm{J}^{imp}_{\Gamma_N} \cdot \bar{\mathrm{F}}_t\, dS - \int_\Omega (\bar{\bar{\mu}}^{-1}\mathrm{M}^{imp}) \cdot (\nabla \times \bar{\mathrm{F}})\, dV \quad \forall\, \mathrm{F} \in H_D(\mathrm{curl};\Omega) \end{array} \right.$$

NUMERICAL RESULTS

Variational Formulation

AXISYMMETRIC PROBLEMS

E_ϕ **-Variational Formulation (Azimuthal)**

$$\begin{cases} \textbf{Find } \boldsymbol{E_\phi} \in \boldsymbol{E_{\phi,D}} + \tilde{\boldsymbol{H}}^1_D(\Omega) \textbf{ such that:} \\ \int_\Omega (\bar{\bar{\mu}}^{-1}_{\rho,z} \nabla \times \mathrm{E}_\phi) \cdot (\nabla \times \bar{\mathrm{F}}_\phi)\, dV - \int_\Omega (\bar{\bar{k}}^2_\phi \mathrm{E}_\phi) \cdot \bar{\mathrm{F}}_\phi \, dV = -j\omega \int_\Omega J^{imp}_\phi \, \bar{F}_\phi \, dV \\ \quad + j\omega \int_{\Gamma_N} J^{imp}_{\phi,\Gamma_N} \, \bar{F}_\phi \, dS - \int_\Omega (\bar{\bar{\mu}}^{-1}_{\rho,z} \mathrm{M}^{imp}_{\rho,z}) \cdot \bar{\mathrm{F}}_\phi \, dV \qquad \forall\, F_\phi \in \tilde{H}^1_D(\Omega) \end{cases}$$

$\mathrm{E}_{\rho,z}$ **-Variational Formulation (Meridian)**

$$\begin{cases} \textbf{Find } (\boldsymbol{E_\rho}, \boldsymbol{E_z}) \in \mathrm{E}_D + \tilde{\boldsymbol{H}}_D(\mathrm{curl};\Omega) \textbf{ such that:} \\ \int_\Omega (\bar{\bar{\mu}}^{-1}_{\phi} \nabla \times \mathrm{E}_{\rho,z}) \cdot (\nabla \times \bar{\mathrm{F}}_{\rho,z})\, dV - \int_\Omega (\bar{\bar{k}}^2_{\rho,z} \mathrm{E}_{\rho,z}) \cdot \bar{\mathrm{F}}_{\rho,z} \, dV = \\ \quad -j\omega \int_\Omega J^{imp}_\rho \bar{F}_\rho + J^{imp}_z \bar{F}_z \, dV + j\omega \int_{\Gamma_N} J^{imp}_{\rho,\Gamma_N} \bar{F}_\rho + J^{imp}_{z,\Gamma_N} \bar{F}_z \, dS \\ \quad - \int_\Omega (\bar{\bar{\mu}}^{-1}_{\phi} \mathrm{M}^{imp}_{\phi}) \cdot \bar{\mathrm{F}}_{\rho,z} \, dV \qquad \forall\, (F_\rho, F_z) \in \tilde{H}_D(\mathrm{curl};\Omega) \end{cases}$$

NUMERICAL RESULTS

Reliability (Can We Trust the Solutions?)

Problem with casing at 10 kHz.

Continuous Elements

Quantity of Interest	Real Part	Imag Part
COARSE GRID	0.1516098429E-08	-0.1456374493E-08
FINE GRID	0.1516094029E-08	-0.1456390824E-08

Edge Elements

Quantity of Interest	Real Part	Imag Part
COARSE GRID	0.1516060872E-08	-0.1456337248E-08
FINE GRID	0.1516093804E-08	-0.1456390864E-08

Error control provided by the fine grid solution.

NUMERICAL RESULTS

Reliability (Can We Trust the Solutions?)

Problem with casing at 10 kHz.

Continuous Elements

Quantity of Interest	Real Part	Imag Part
COARSE GRID	0.1516098429E-08	-0.1456374493E-08
FINE GRID	0.1516094029E-08	-0.1456390824E-08

Edge Elements

Quantity of Interest	Real Part	Imag Part
COARSE GRID	0.1516060872E-08	-0.1456337248E-08
FINE GRID	0.1516093804E-08	-0.1456390864E-08

Comparison between continuous elements vs. edge elements.

NUMERICAL RESULTS

Accuracy (Are the Solutions Accurate?)

Problem with Casing (Convergence Curve)

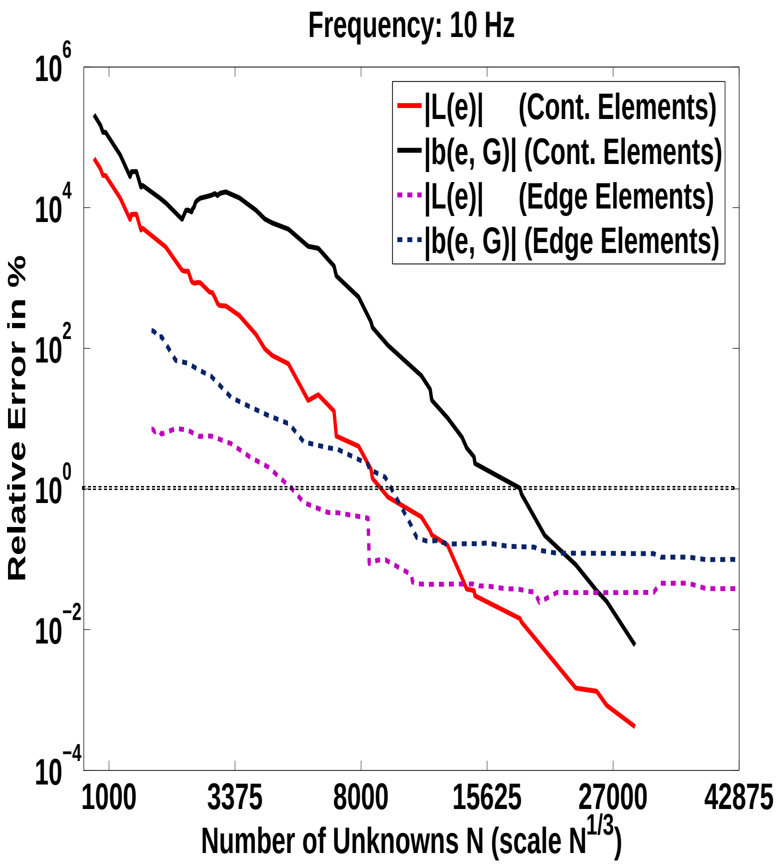

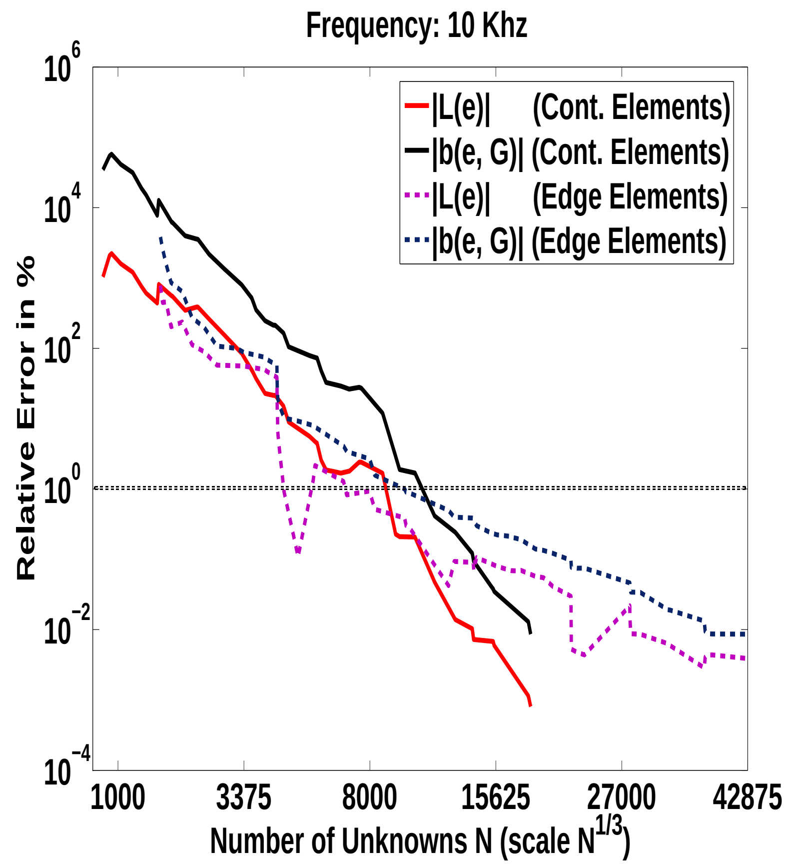

EXTREMELY ACCURATE SOFTWARE

NUMERICAL RESULTS

Performance (How Fast Can We Solve the Problems?)

80 Vert. Pos.	$10^{-6}\Omega\cdot m$	$10^{-5}\Omega\cdot m$
Toroid (10 Khz)	19' 46"	16' 28"
Ring of Vert. Dipoles (10 Khz)	22' 47"	17' 02"
Ring of Horiz. Dipoles (10 Khz)	19' 25"	13' 25"
Electrodes (0 Hz)	10' 10"	8' 35"

IBM Power 4 compiler 1.3 Ghz (4 years old)

Possible improvements in performance:

- **To use a 3.4 Ghz processor.**
- **To execute the code in 8 processors (10 positions per processor).**
- **To improve implementation.**

HIGH PERFORMANCE SOFTWARE

SIMULATION OF LOGGING INSTRUMENTS

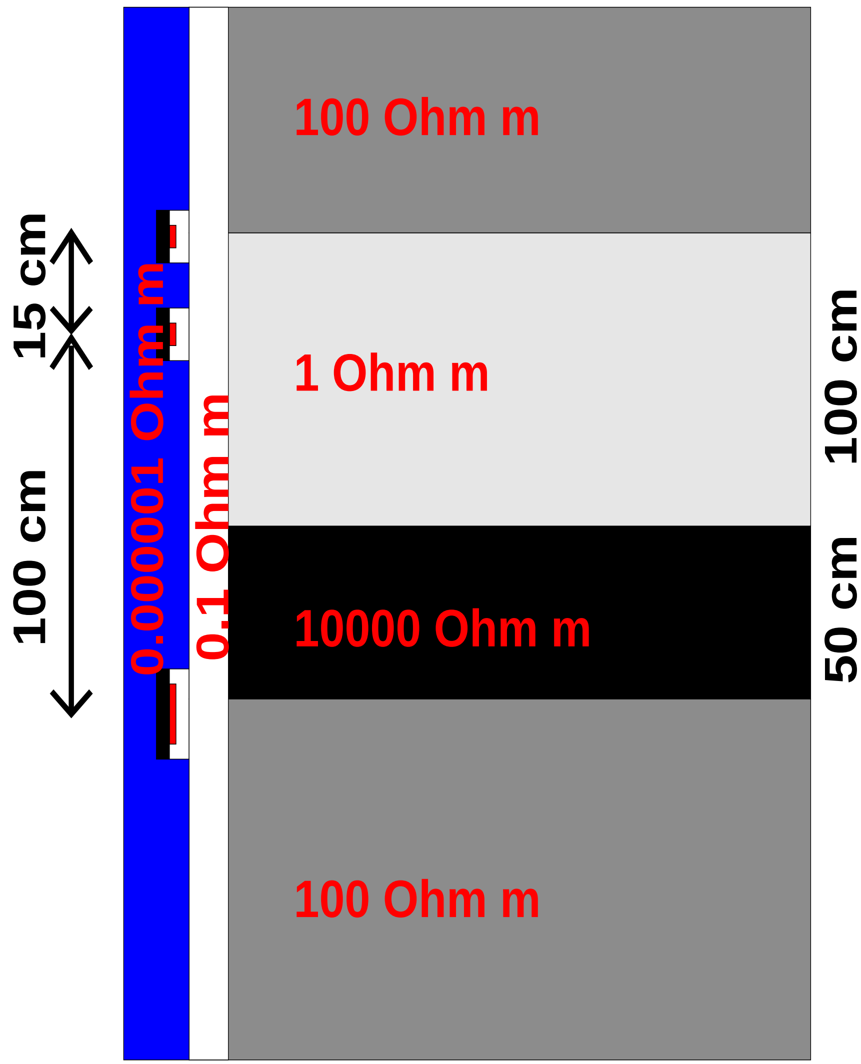

Description of Antennas

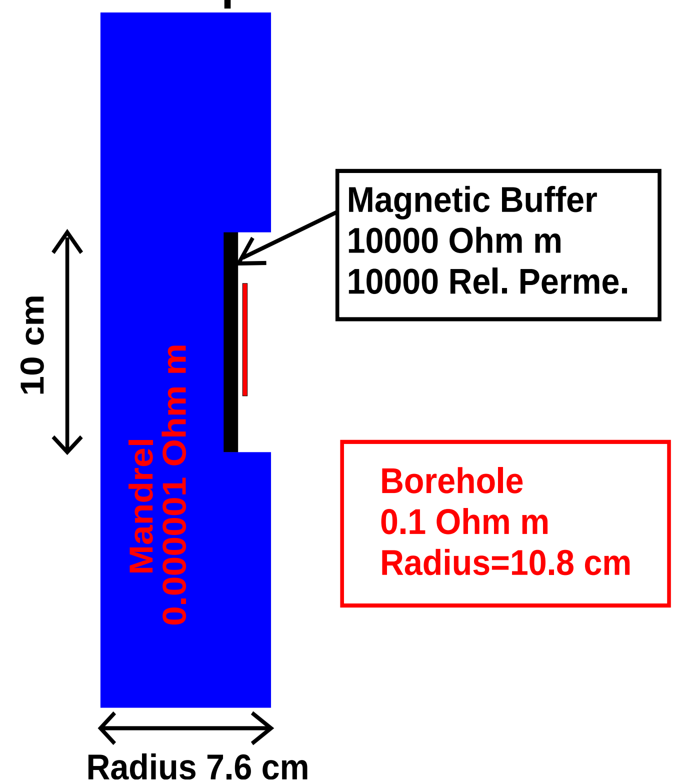

Goal: To Compute First Difference of Potential on Receiving Antennas

SIMULATION OF LOGGING INSTRUMENTS

First. Vert. Diff. E_ϕ (solenoid). Position: 0.475m

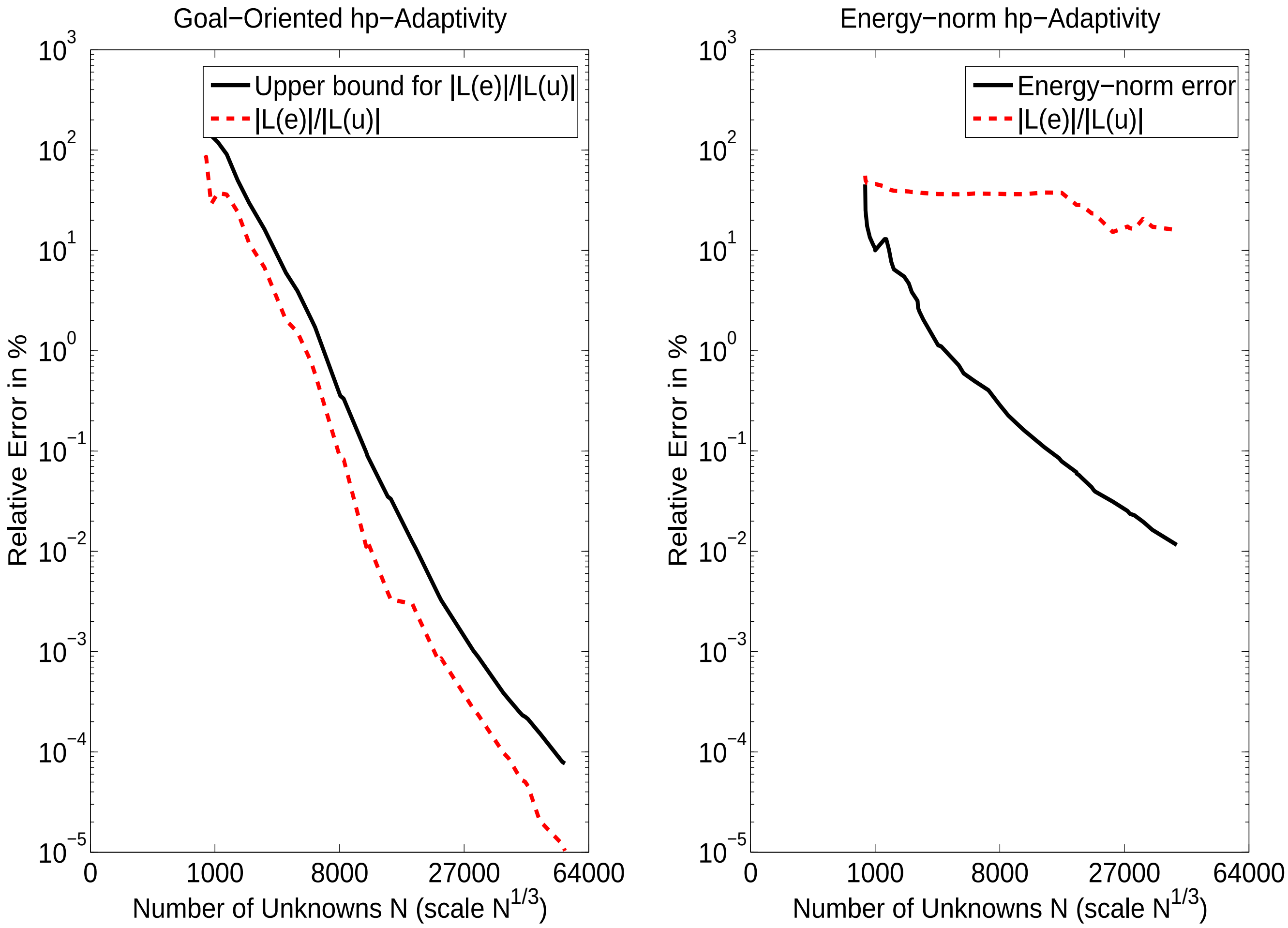

SIMULATION OF LOGGING INSTRUMENTS

Goal-Oriented vs. Energy-norm hp-Adaptivity

Problem with Mandrel at 2 Mhz.

Continuous Elements (Goal-Oriented Adaptivity)

Quantity of Interest	Real Part	Imag Part
COARSE GRID	-0.1629862203E-01	-0.4016944732E-02
FINE GRID	-0.1629862347E-01	-0.4016944223E-02

Continuous Elements (Energy-norm Adaptivity)

Quantity of Interest	Real Part	Imag Part
0.01% ENERGY ERROR	-0.1382759158E-01	-0.2989492851E-02

It is critical to use GOAL-ORIENTED adaptivity.

SIMULATION OF LOGGING INSTRUMENTS

First. Vert. Diff. E_ϕ (solenoid). Position: 0.475m

ENERGY-NORM HP-ADAPTIVITY

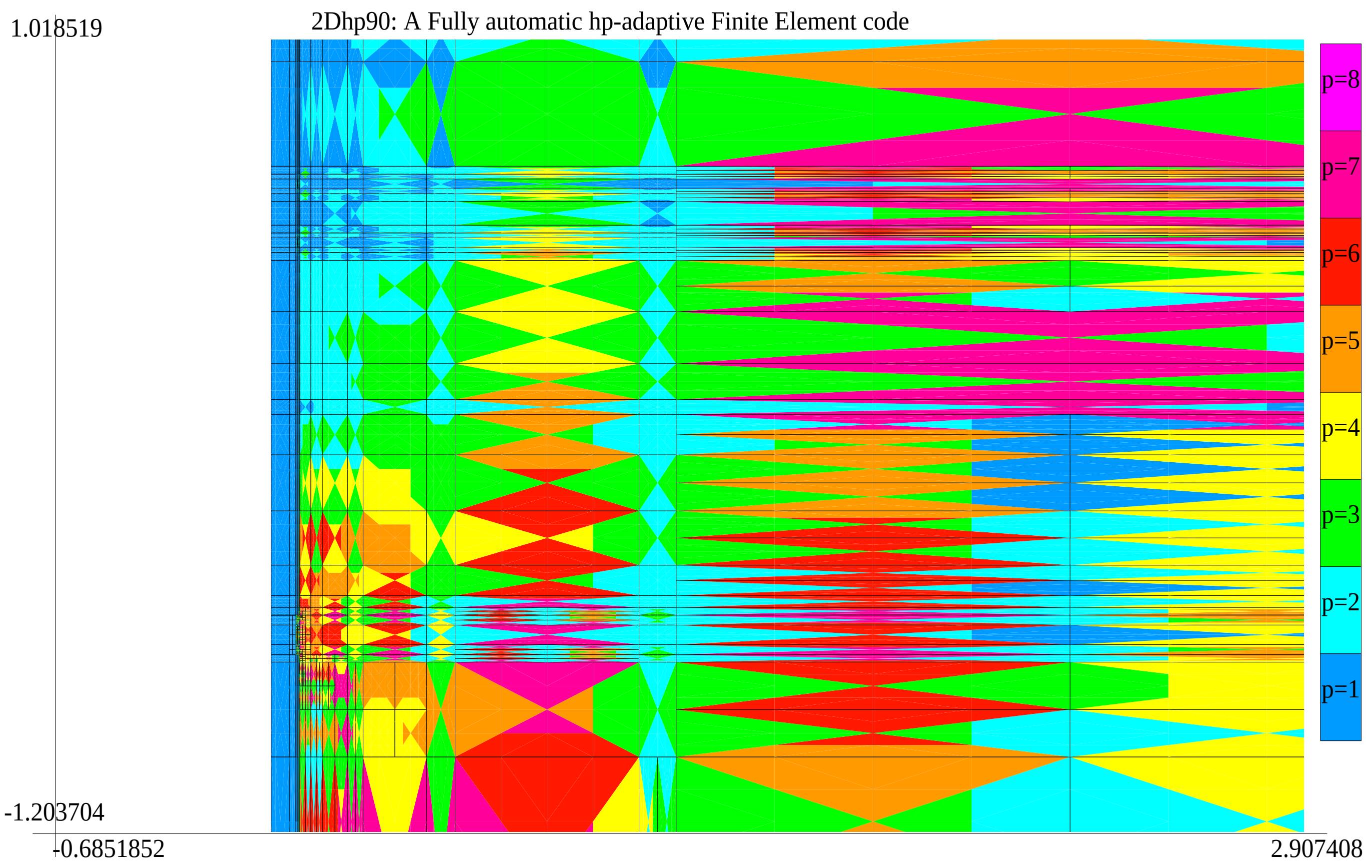

SIMULATION OF LOGGING INSTRUMENTS

First. Vert. Diff. E_ϕ (solenoid). Position: 0.475m

GOAL-ORIENTED HP-ADAPTIVITY

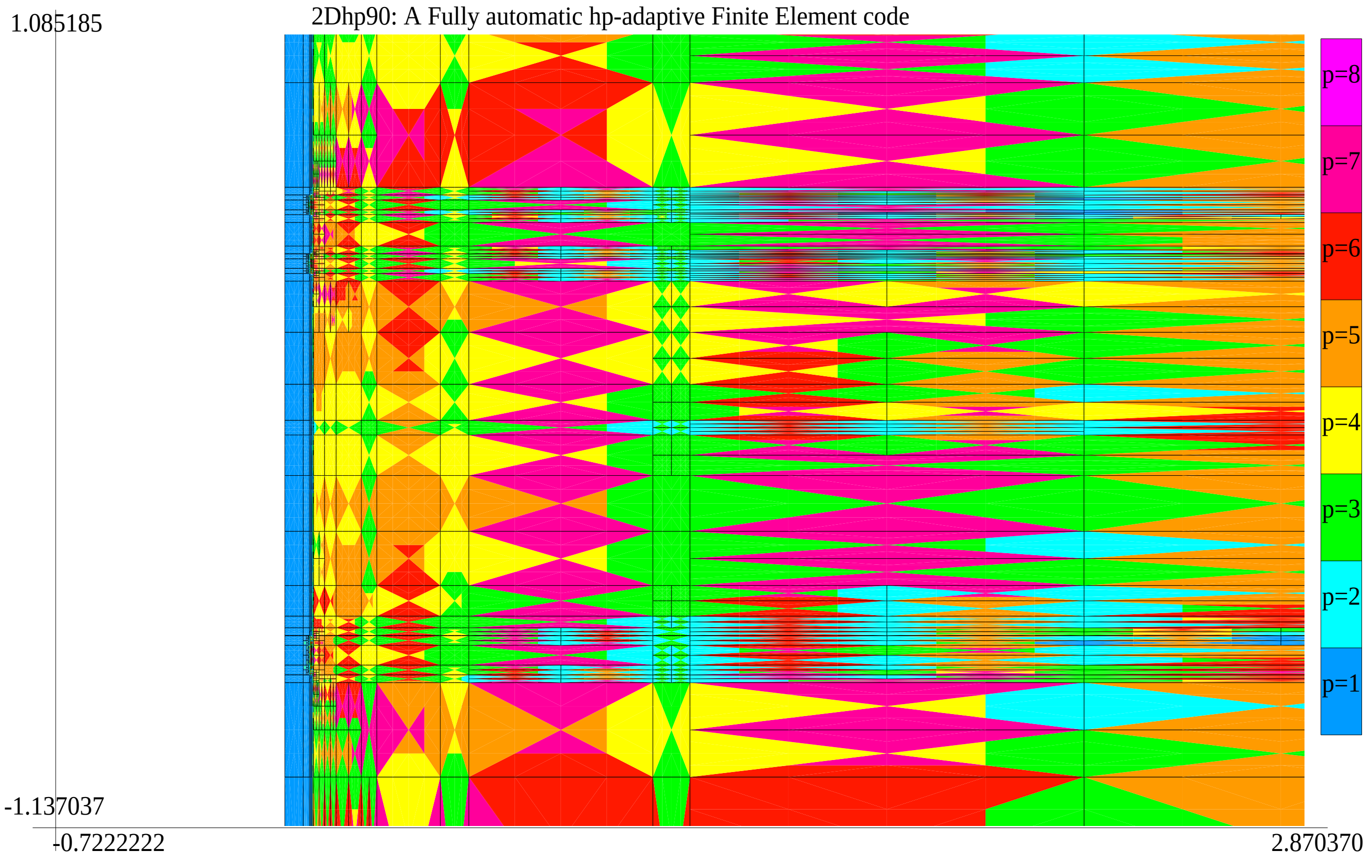

SIMULATION OF LOGGING INSTRUMENTS

First. Vert. Diff. E_ϕ (solenoid). Position: 0.475m

GOAL-ORIENTED HP-ADAPTIVITY (ZOOM TOWARDS FIRST RECEIVER ANTENNA)

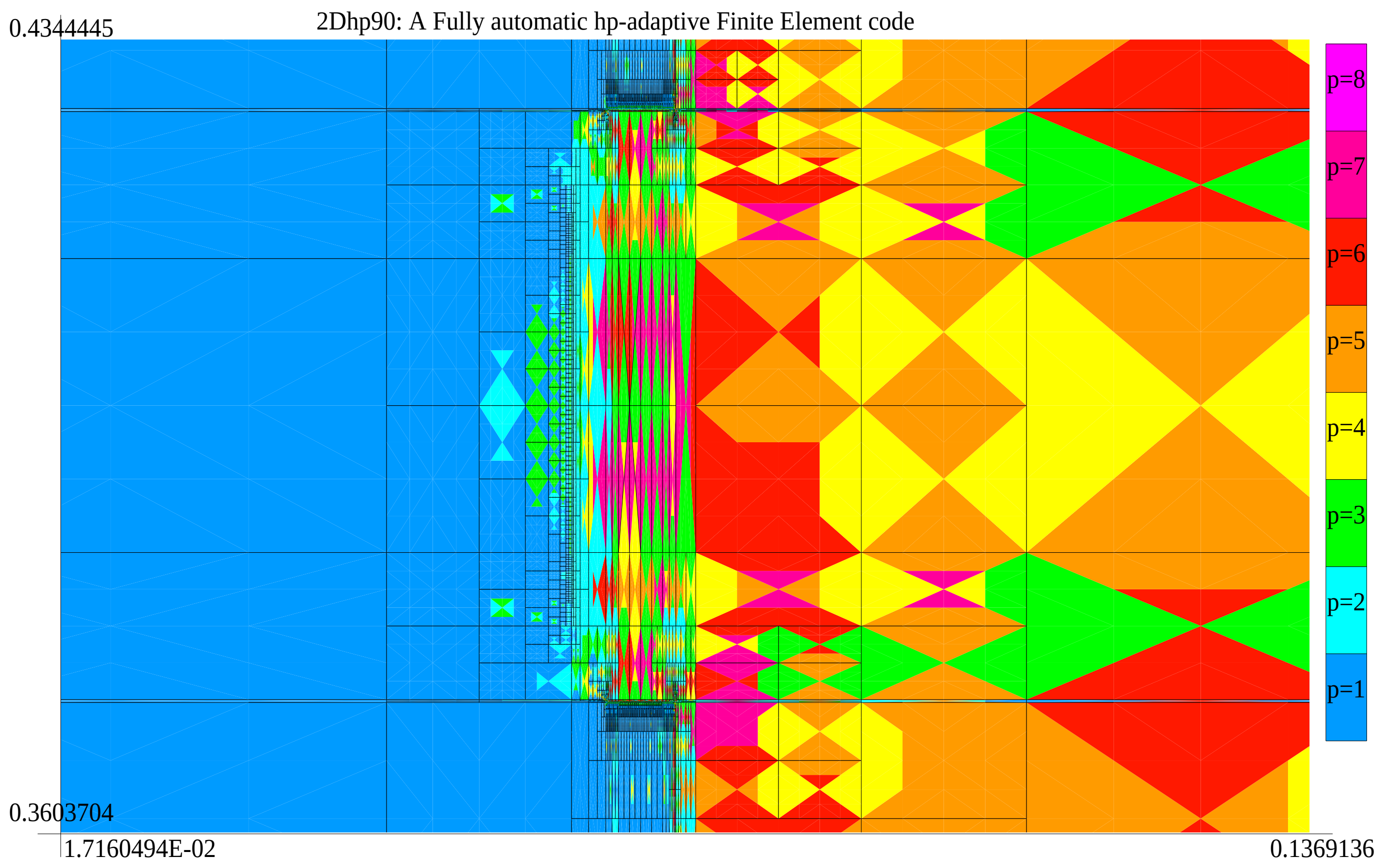

SIMULATION OF LOGGING INSTRUMENTS

E_ϕ for a solenoid antenna

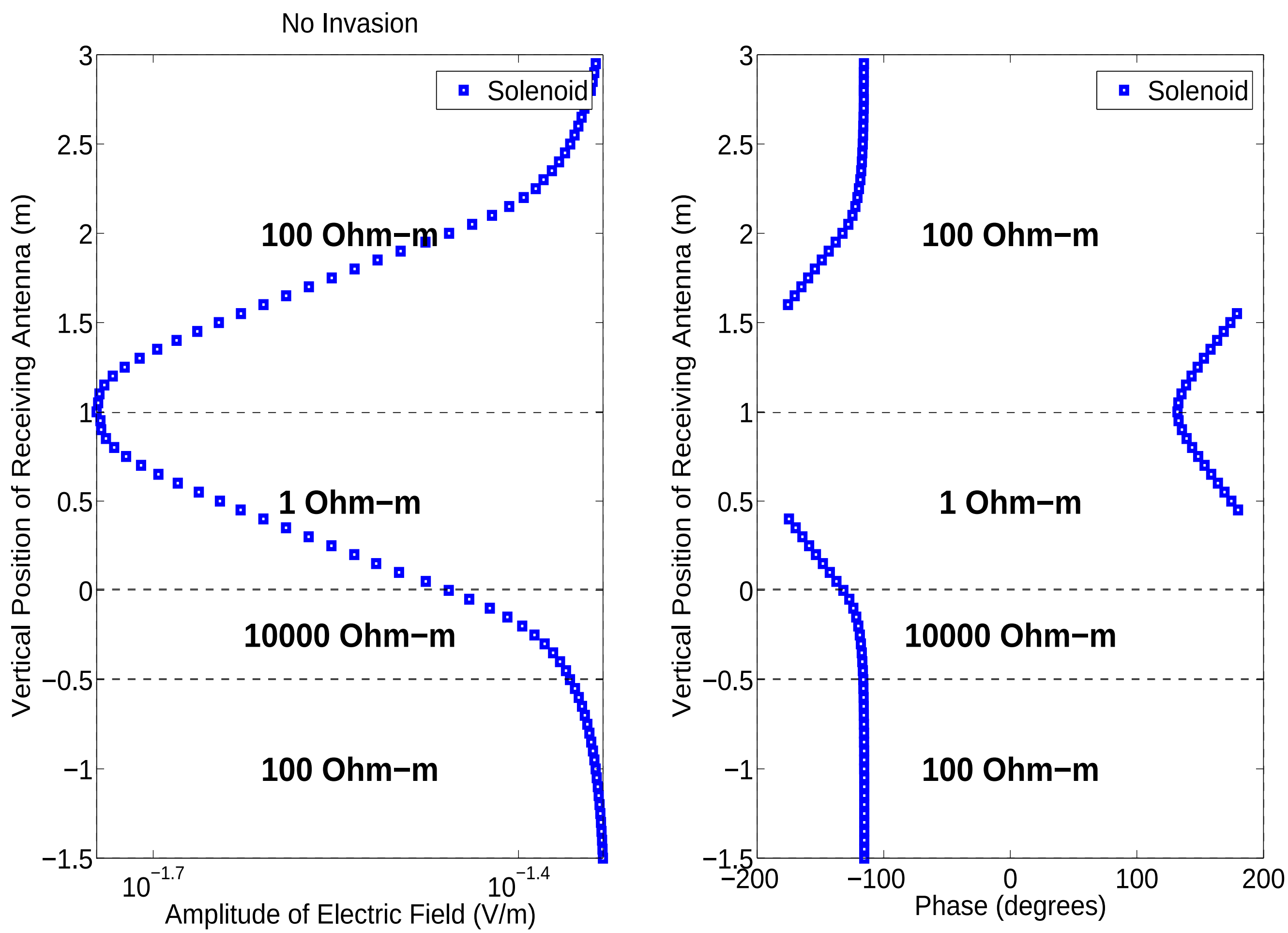

SIMULATION OF LOGGING INSTRUMENTS

H_ϕ for different antennas

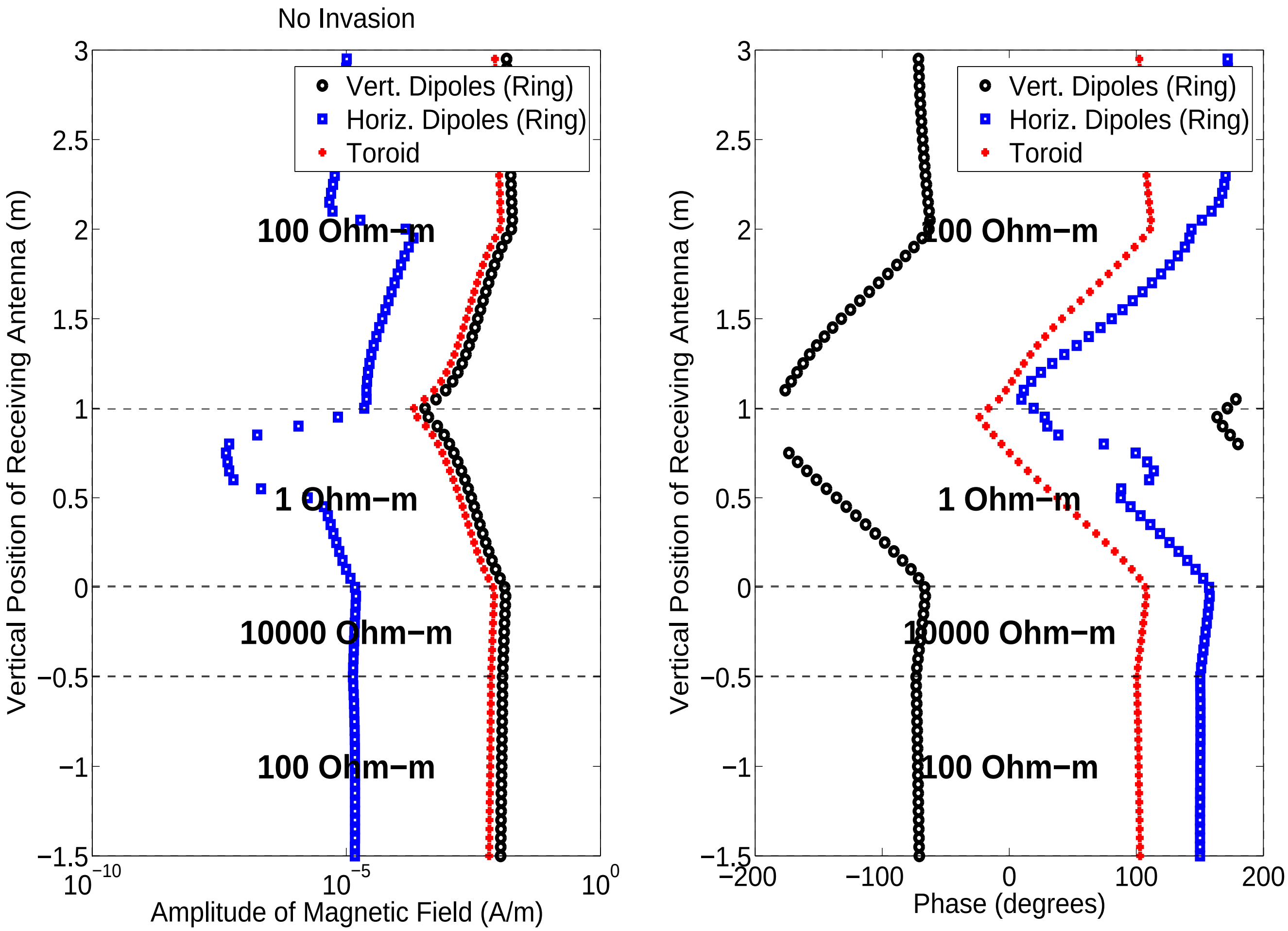

SIMULATION OF LOGGING INSTRUMENTS

First Vert. Diff. H_ϕ for different antennas

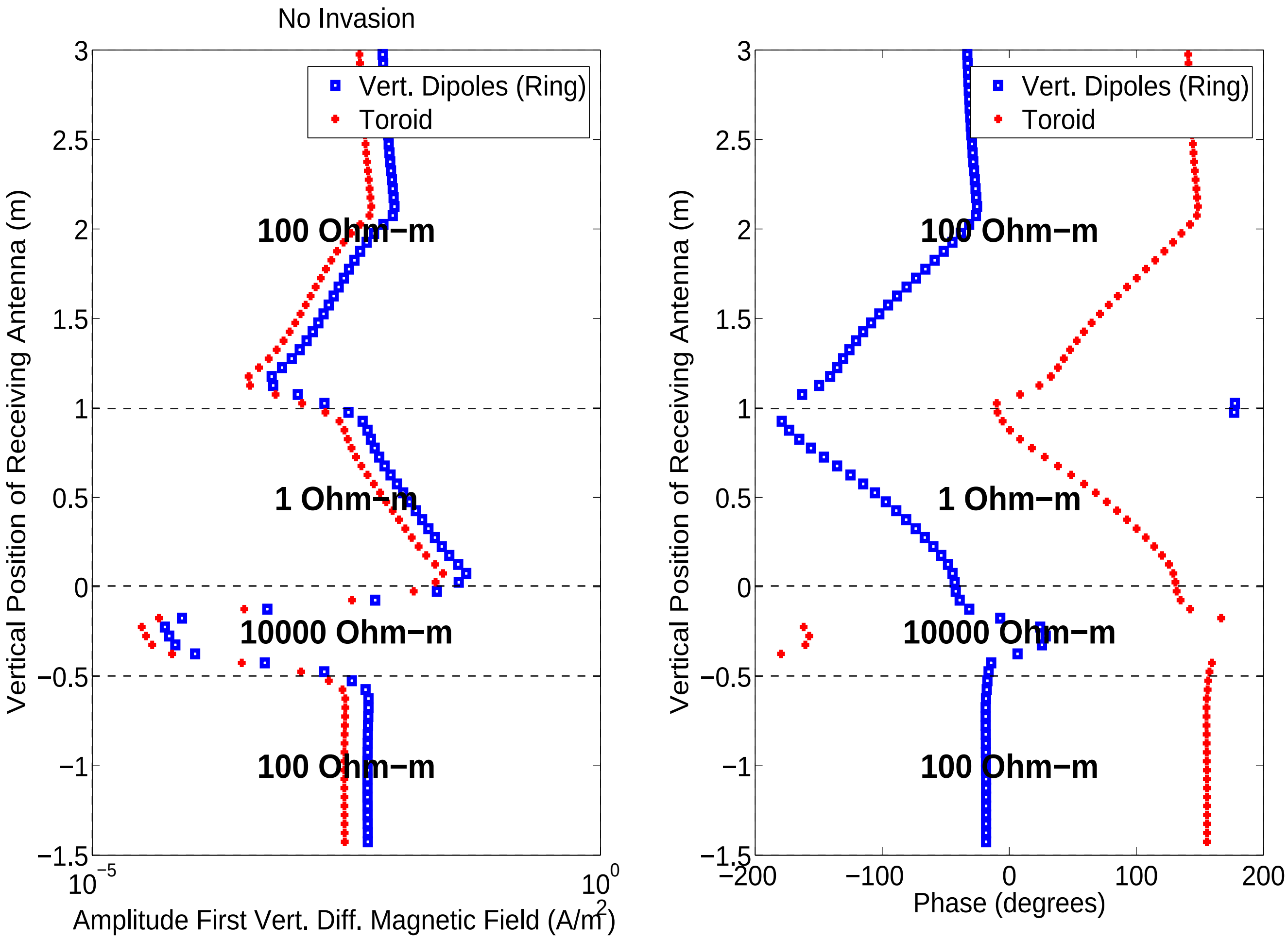

SIMULATION OF LOGGING INSTRUMENTS

First Vert. Diff. E_z for a toroid antenna

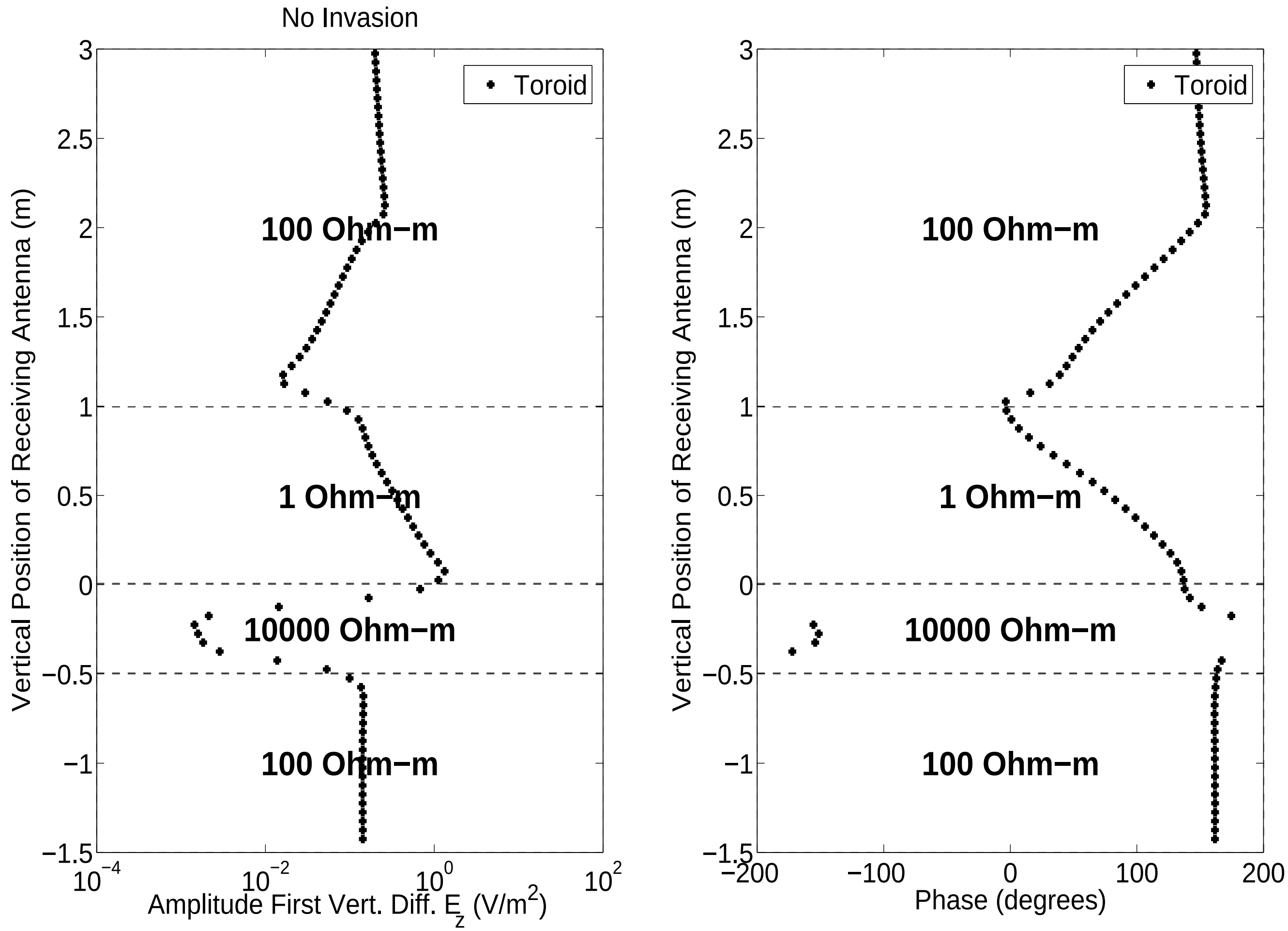

SIMULATION OF LOGGING INSTRUMENTS

First Vert. Diff. H_z for a solenoid antenna

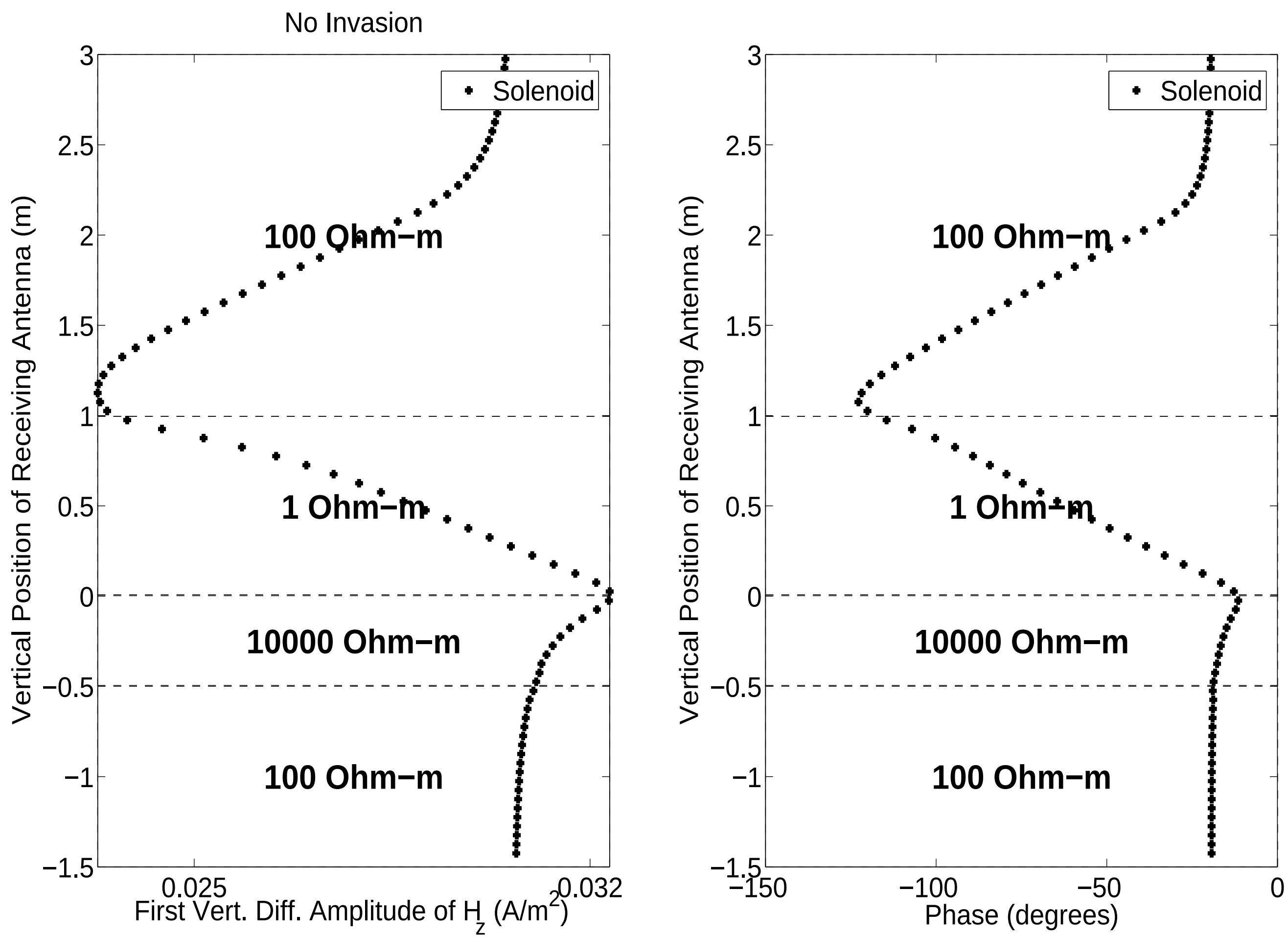

SIMULATION OF LOGGING INSTRUMENTS

First Vert. Diff. E_ϕ for a solenoid antenna

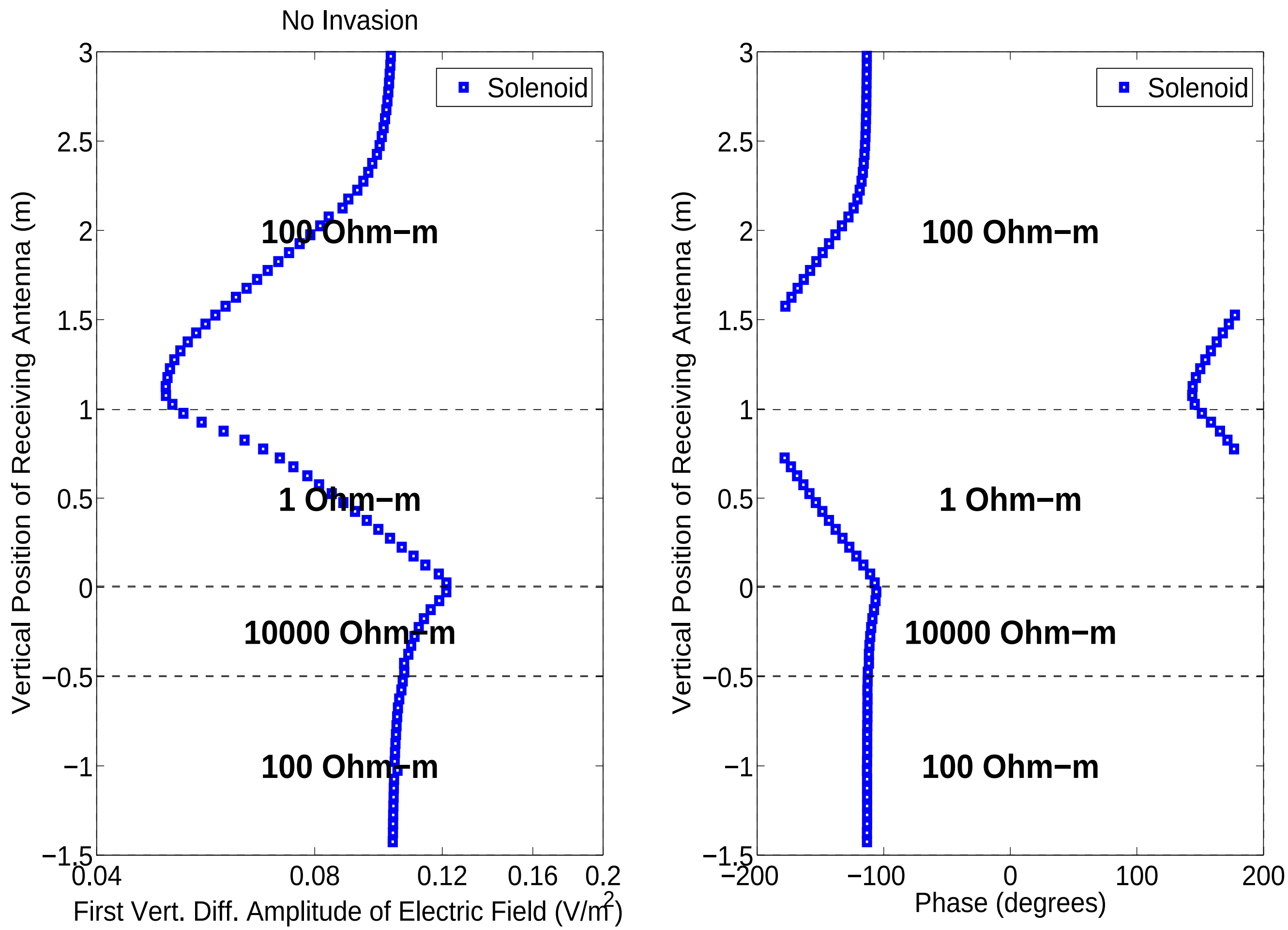

SIMULATION OF LOGGING INSTRUMENTS

Use of Magnetic Buffers (E_ϕ for a solenoid)

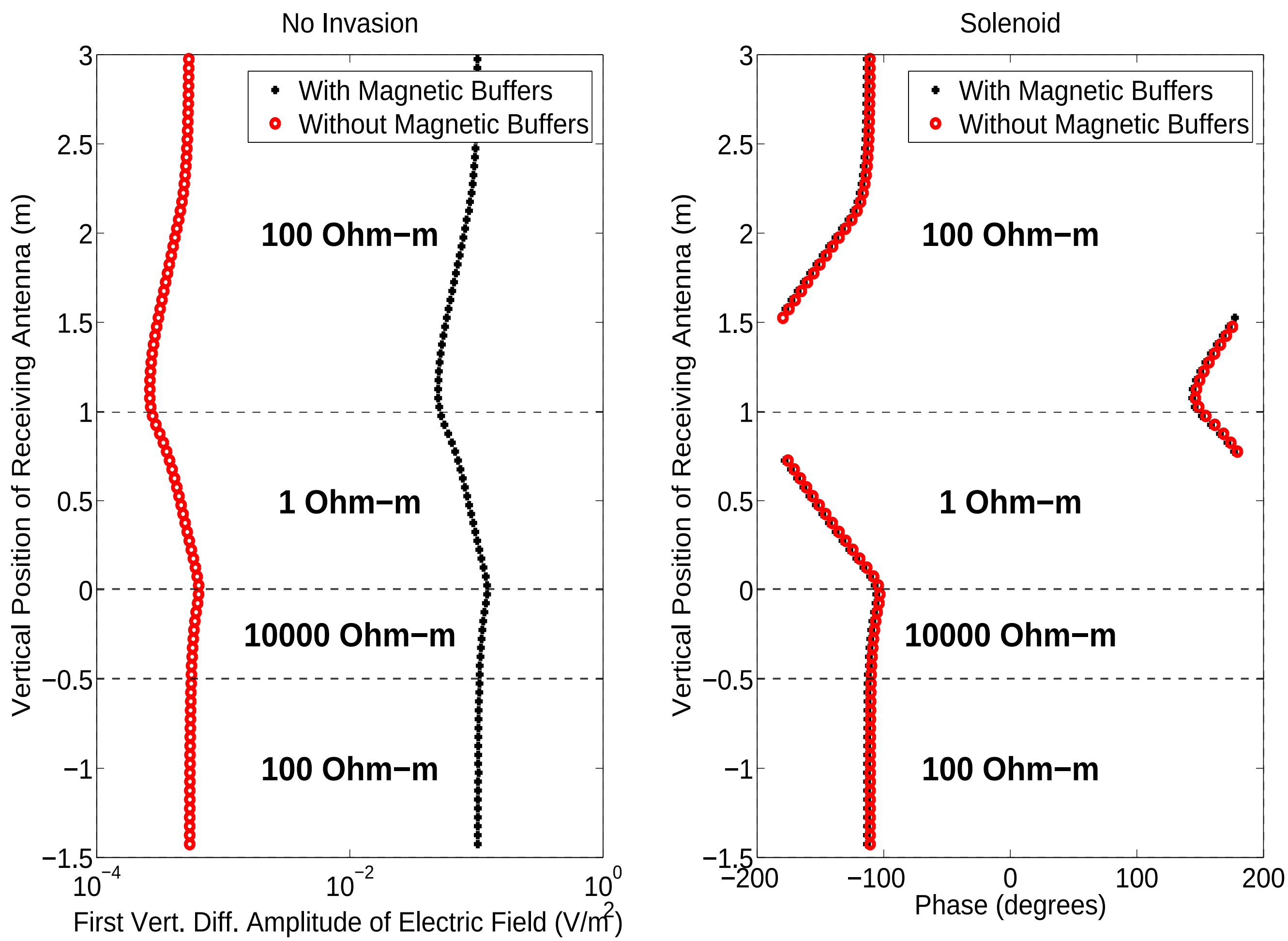

SIMULATION OF LOGGING INSTRUMENTS

Use of Magnetic Buffers (H_ϕ for a toroid)

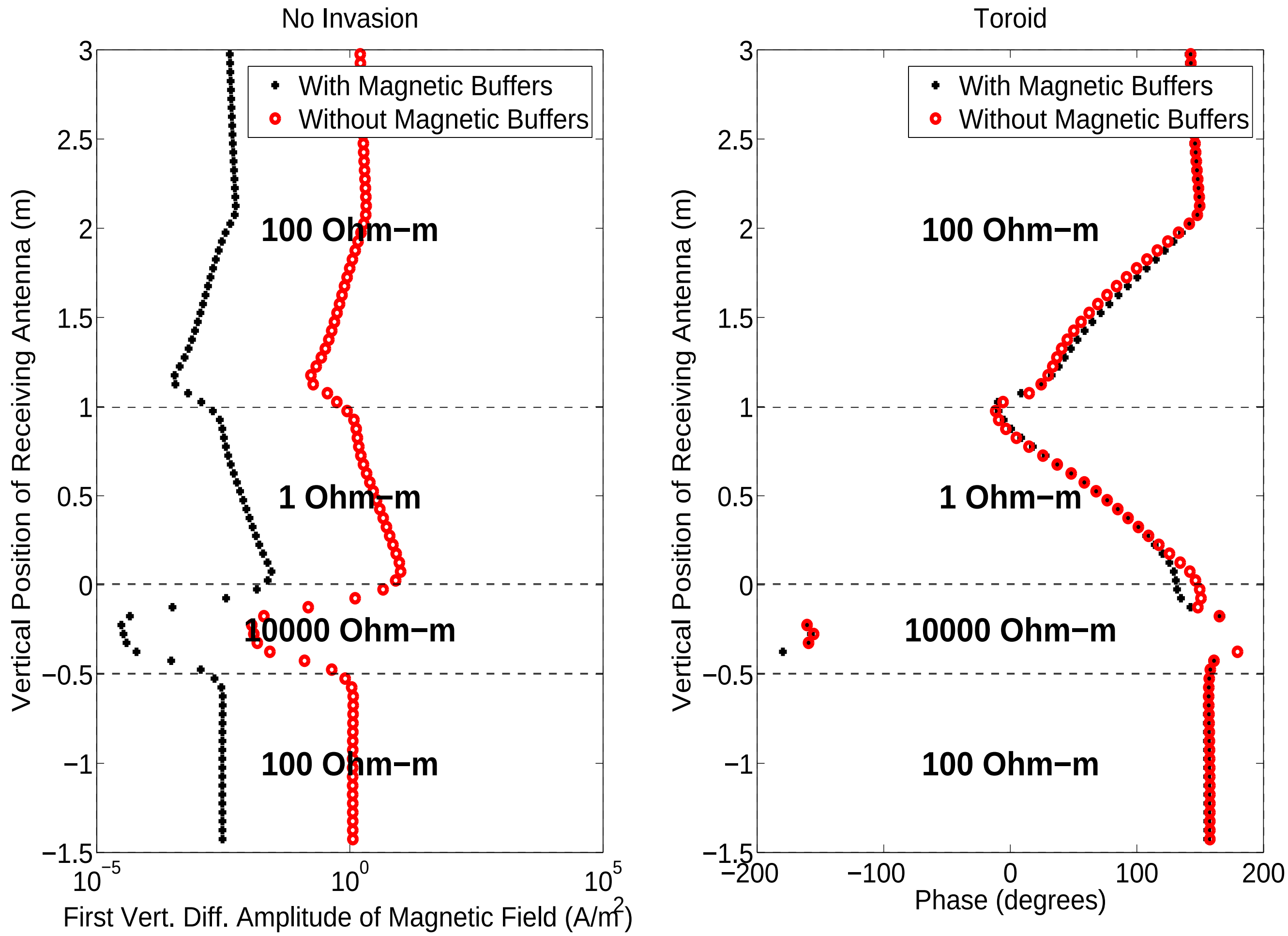

SIMULATION OF LOGGING INSTRUMENTS

Invasion study (E_ϕ for a solenoid)

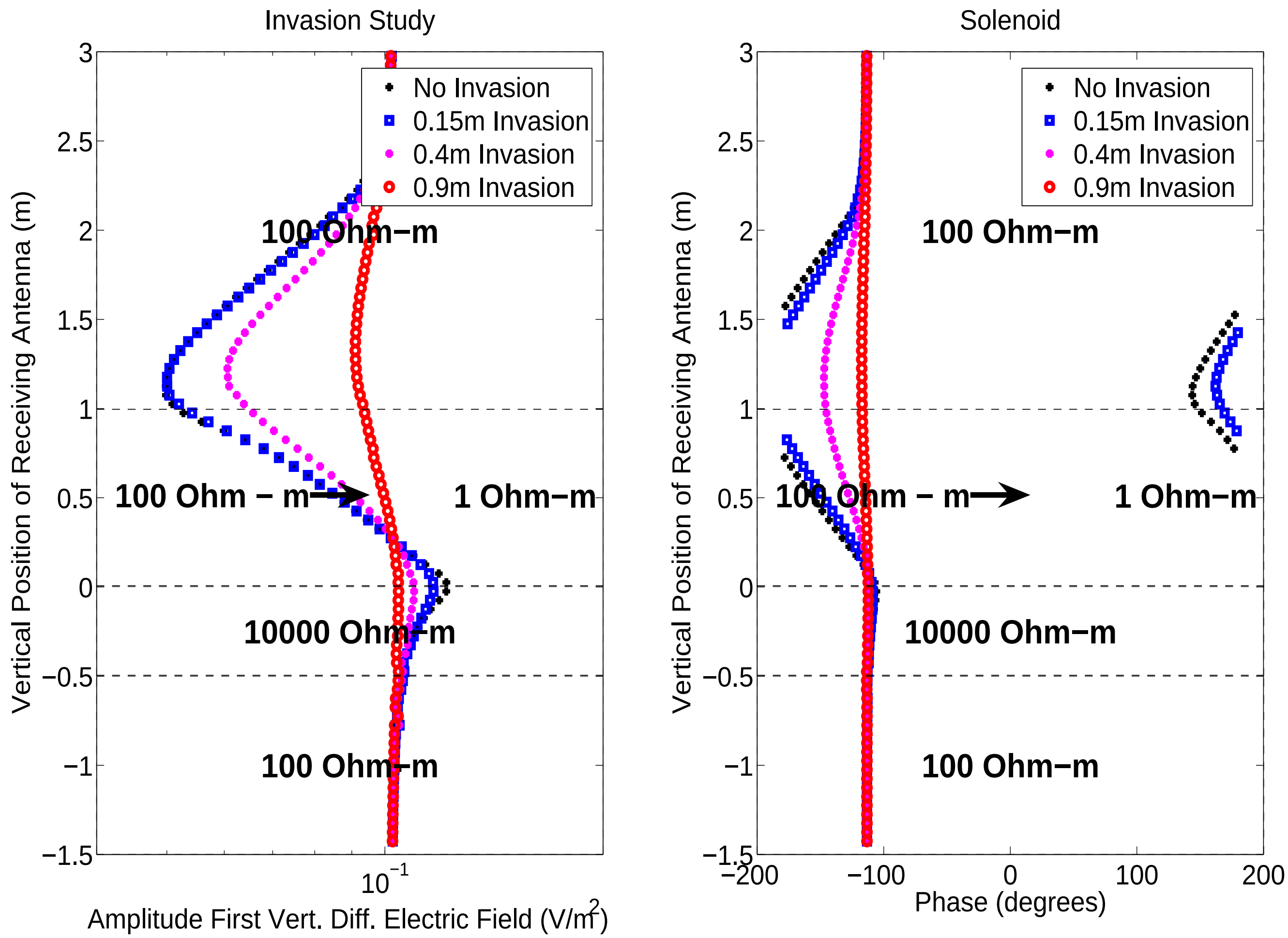

SIMULATION OF LOGGING INSTRUMENTS

Invasion study (H_ϕ for a toroid)

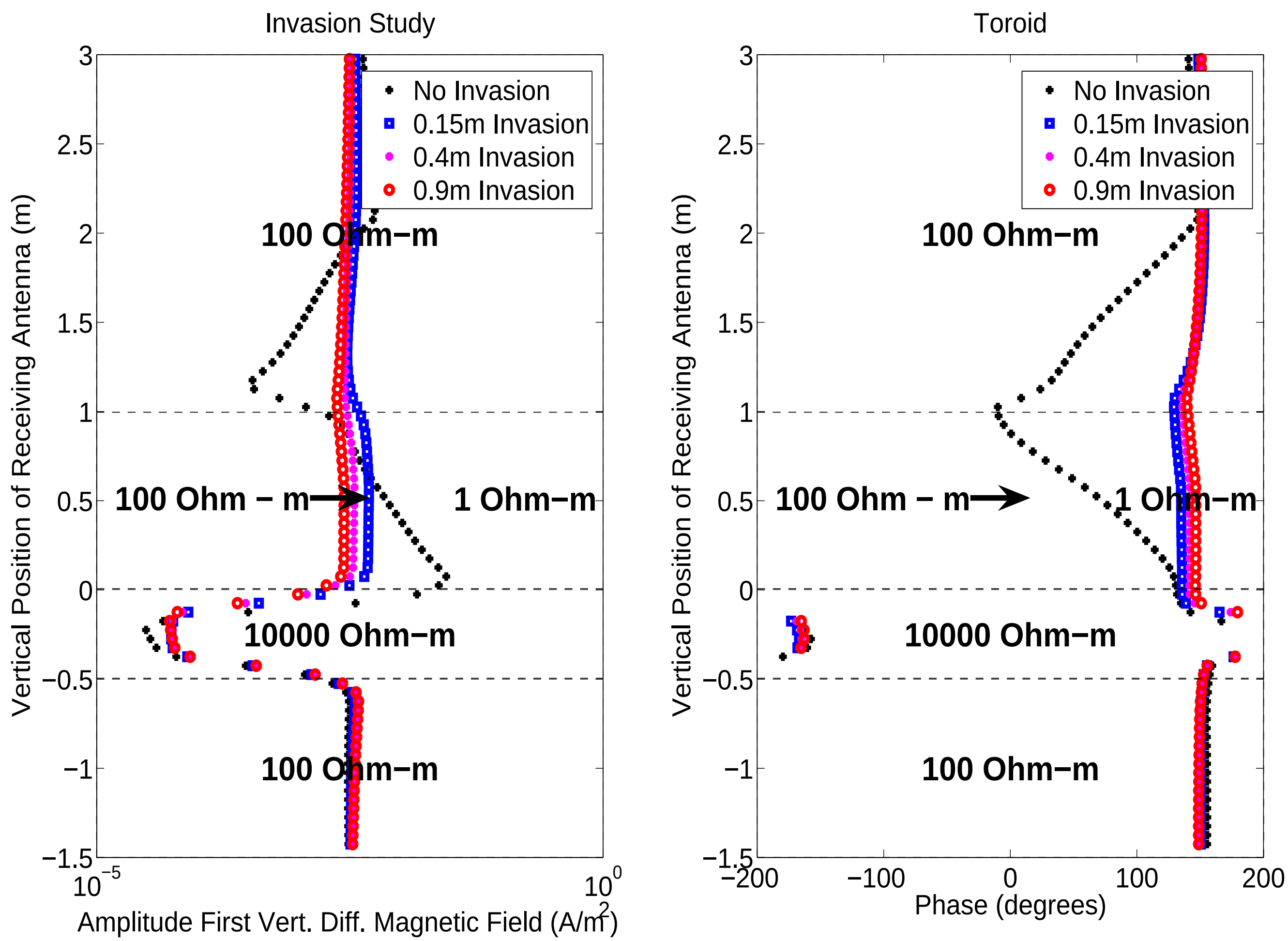

SIMULATION OF LOGGING INSTRUMENTS

Invasion study (E_ϕ for a solenoid)

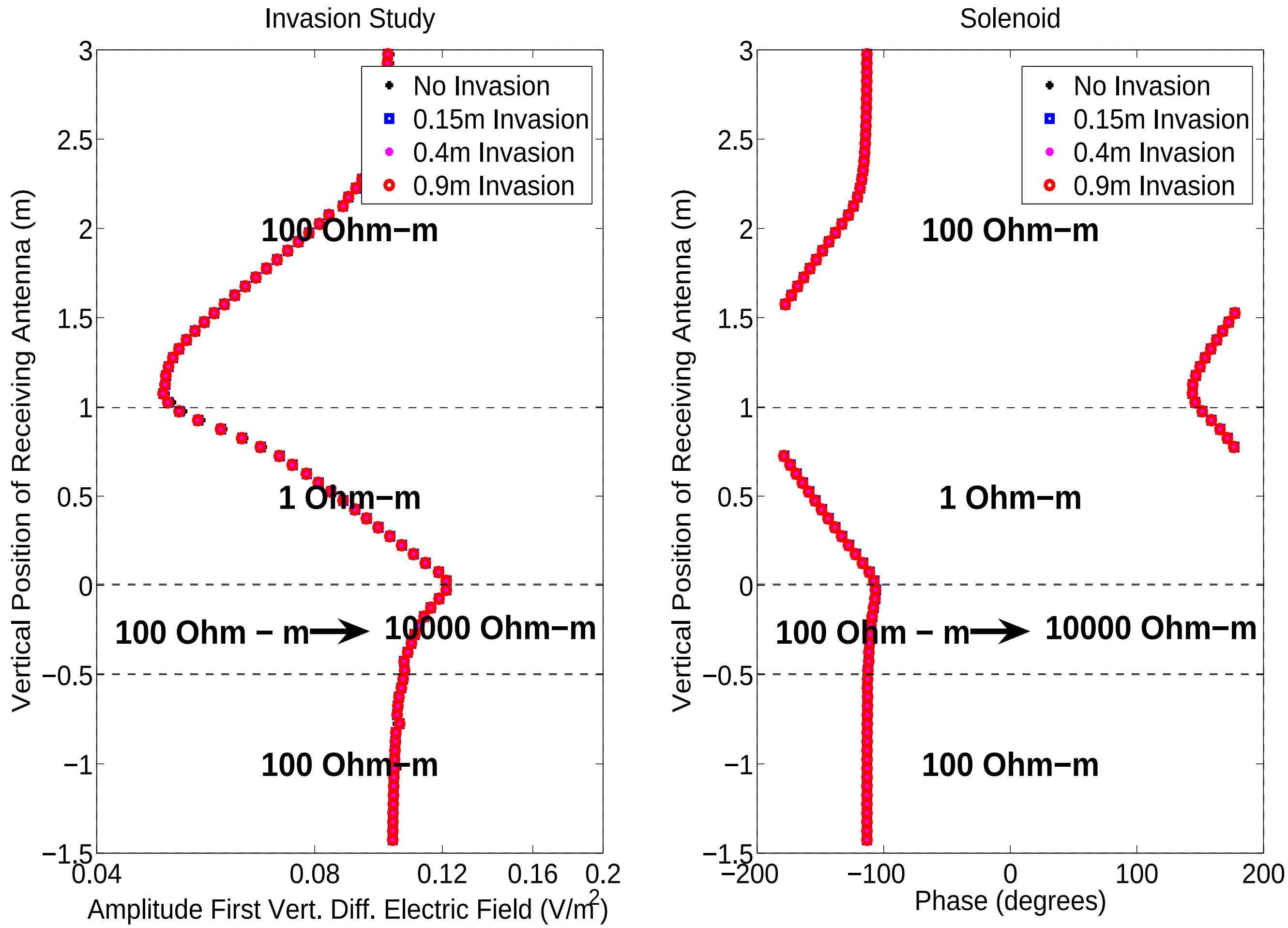

SIMULATION OF LOGGING INSTRUMENTS

Invasion study (H_ϕ for a toroid)

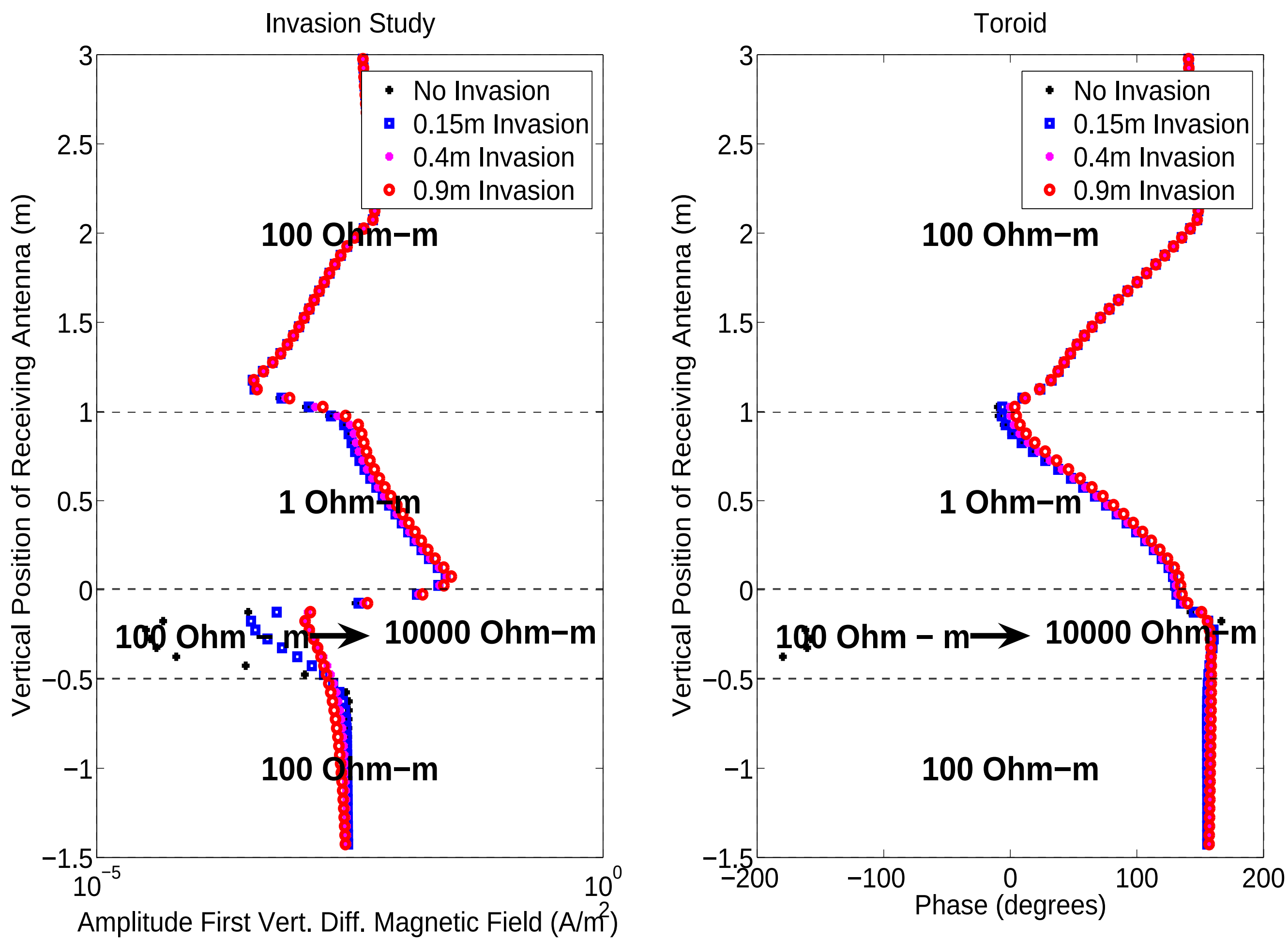

SIMULATION OF LOGGING INSTRUMENTS

Invasion and mandrel magnetic permeab. (E_ϕ)

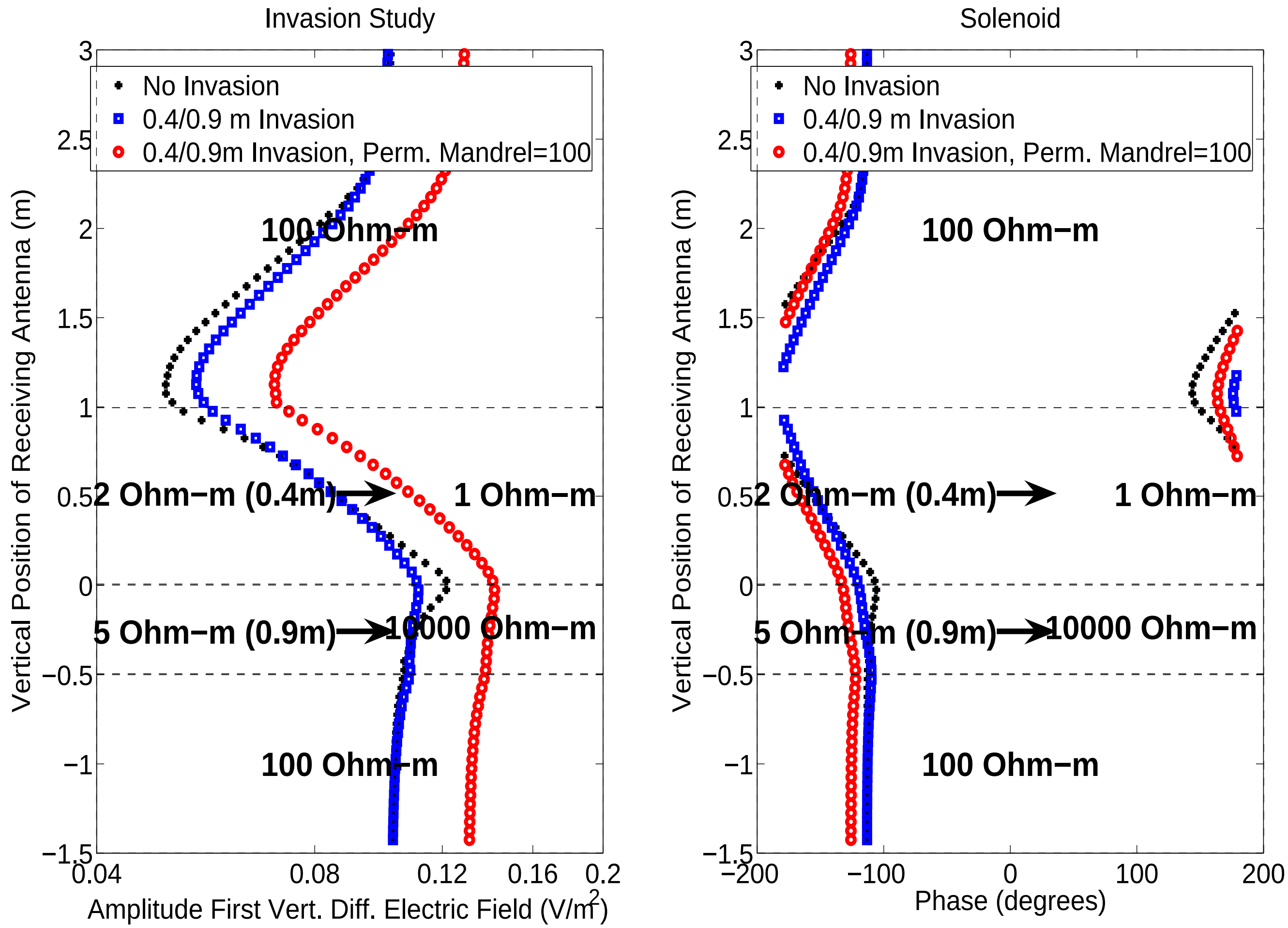

SIMULATION OF LOGGING INSTRUMENTS

Invasion and mandrel magnetic permeab. (H_ϕ)

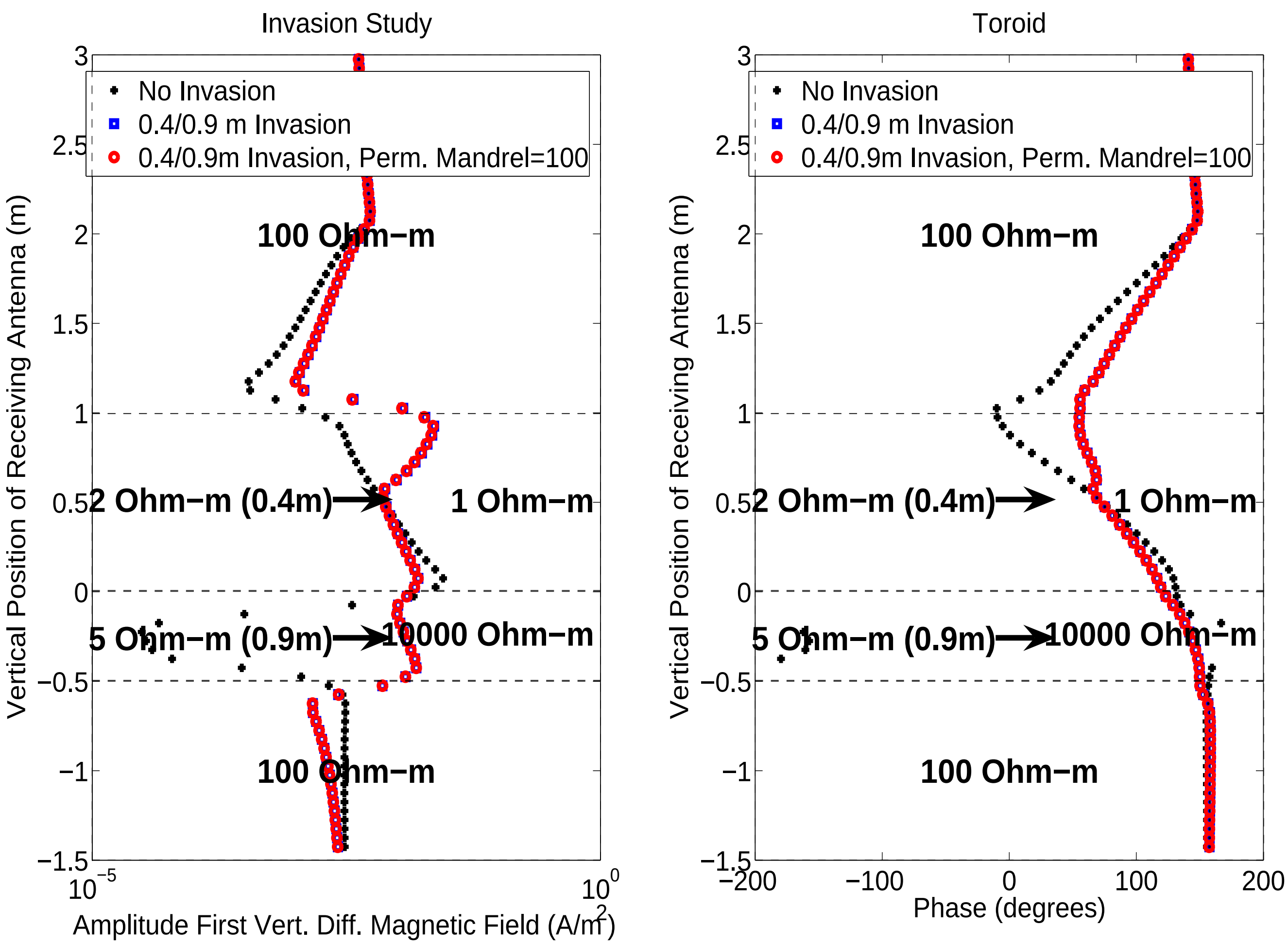

SIMULATION OF LOGGING INSTRUMENTS

Anisotropy (H_ϕ)

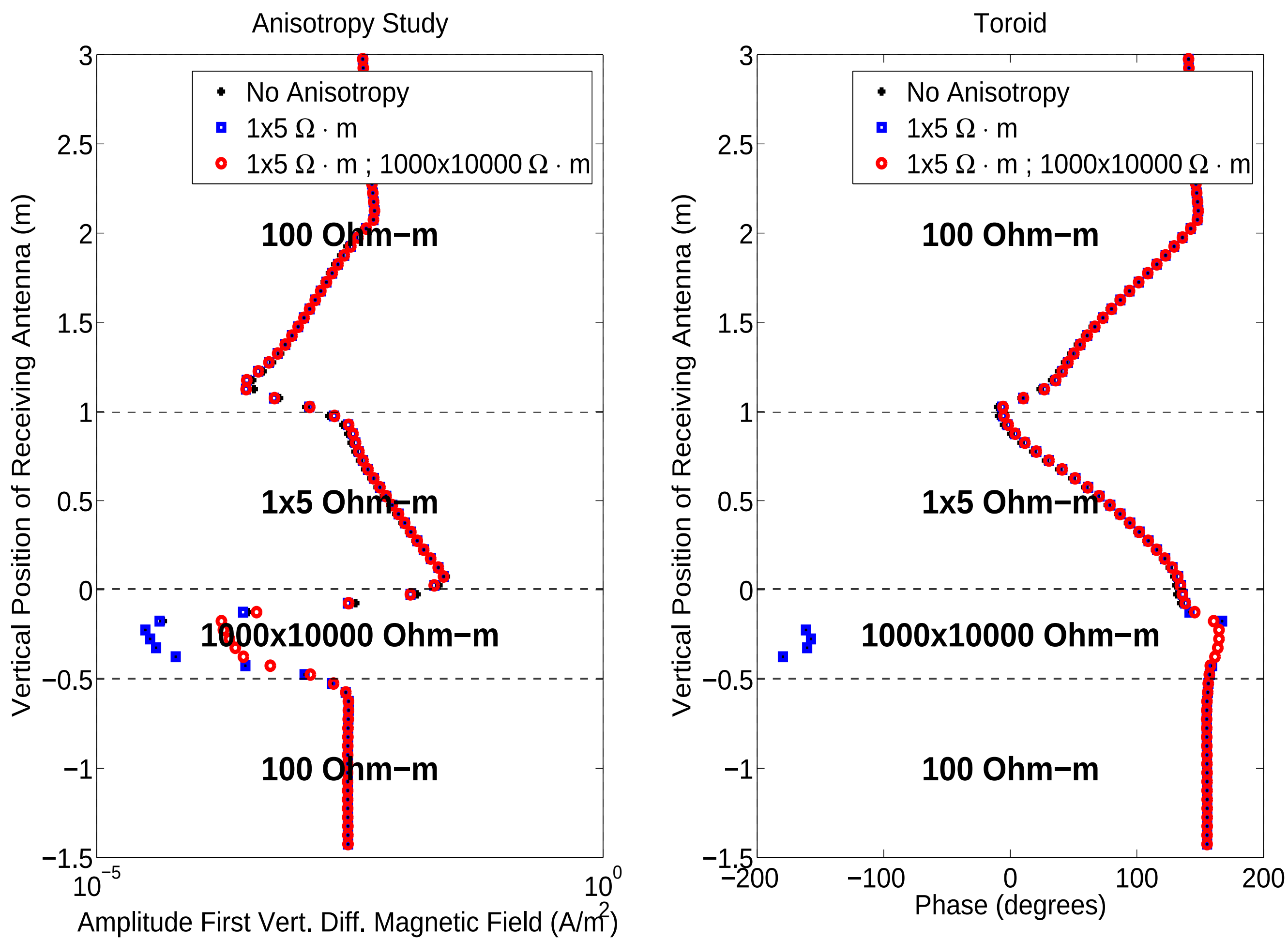

CONCLUSIONS AND FUTURE WORK

- **The self-adaptive goal-oriented hp-adaptive strategy converges exponentially in terms of a user-prescribed quantity of interest vs. the CPU time.**
- **We obtain fast, reliable and accurate solutions for problems with a large dynamic range and high material constrasts.**

Future Work

- **To apply the self-adaptive goal-oriented hp-FEM to 3D problems for simulation of deviated wells.**
- **To apply the self-adaptive goal-oriented hp-FEM for inversion of 2D multi-physic problems.**